DIAGNOSTICS OF A PLASMA FLAME EXHAUSTING TO ATMOSPHERIC PRESSURE

By

W. K. McGregor, Jr., M. T. Dooley, and L. E. Brewer

Rocket Test Facility
ARO, INC.

January 1962

ARNOLD ENGINEERING DEVELOPMENT CENTER
AIR FORCE SYSTEMS COMMAND
UNITED STATES AIR FORCE

NOTICES

Qualified requesters may obtain copies of this report from ASTIA. Orders will be expedited if placed through the librarian or other staff member designated to request and receive documents from ASTIA.

When Government drawings, specifications or other data are used for any purpose other than in connection with a definitely related Government procurement operation, the United States Government thereby incurs no responsibility nor any obligation whatsoever; and the fact that the Government may have formulated, furnished, or in any way supplied the said drawings, specifications, or other data, is not to be regarded by implication or otherwise as in any manner licensing the holder or any other person or corporation, or conveying any rights or permission to manufacture, use, or sell any patented invention that may in any way be related thereto.

DIAGNOSTICS OF A PLASMA FLAME EXHAUSTING TO ATMOSPHERIC PRESSURE

By

W. K. McGregor, Jr., M. T. Dooley, and L. E. Brewer

Rocket Test Facility

ARO, INC.

a subsidiary of Sverdrup and Parcel, Inc.

January 1962

Program Area 806A, Project 8951, Task 89104
ARO Project No. 150927

Contract No. AF 40(600)-800 S/A 24(61-73)

ABSTRACT

A spectrometric method to measure temperature in a high temperature gas stream produced by a Gerdien-type arc plasma generator was developed. The Fowler-Milue peaking function method was employed which utilized both the spectral line and continuum radiation in the 4000 Å range from an argon plasma. Excitation temperatures measured from line radiation and electron temperatures determined from the continuum radiation agreed within about five percent. The method was found to be applicable provided temperatures larger than 16,000°K existed at the center of the axisymmetric jet; the range of temperature measurement was then from about 7000 to 28,000°K.

Comparison of the average temperature obtained using the spectrometric method with the average temperature obtained using an energy balance indicated serious disagreement. Comparison of the total enthalpy obtained using the spectral temperature with that obtained from the energy balance also indicated disagreement. It was then shown that the reason for the disagreement was that the jet consisted of high frequency arc channels moving about in the stream and that the radiant emission resulted from these high temperature electrons rather than from the average gas atoms. Thus, the temperature measured was that of the electrons and was not the average gas temperature.

CONTENTS

TABLES

ILLUSTRATIONS

NOMENCLATURE

A	Total cross-sectional area of axisymmetric jet
$A_{nn'}$	The Einstein transition probability of spontaneous emission
$B_{nn'}$	The Einstein transition probability of induced emission
$B_{n'n}$	The Einstein transition probability of induced absorption
c	Velocity of light
$D(\nu_{nn'})$	The number of photons per unit volume (energy density) having frequency, $\nu_{nn'}$
$E_{o,n}$	The n^{th} quantum state of the un-ionized species
$E_{r,n}$	The n^{th} quantum energy state of species, r
$F(x)$	Measured quantity of radiation at a position, x, along a line parallel to the radius of the axisymmetric jet
$g_n, g_{n'}$	Statistical weight, $2J + 1$, where J is the orbital quantum number of the n and n' states, respectively
$g_{r,n}$	Statistical weight of n^{th} quantum state and r^{th} species
h^*	Specific enthalpy
h	Planck's constant
$I_{bb}(\nu_{nn'})$	The intensity of radiation of the spectral line at frequency, $\nu_{nn'}$
$I_{fb}(\nu)$	The intensity of the continuous radiation at frequency, ν, resulting from free-bound transitions
$I_{ff}(\nu)$	The intensity of the continuous radiation at frequency, ν, resulting from free-free transitions
$I(r)$	Quantity of radiation at a radius, r, from the center of the axisymmetric jet found from the inversion of the measured function, $F(x)$
J	Orbital quantum number
K	Defined constant
k	Boltzmann's constant
m_e	Mass of the electron
$N_0, N_1, N_2 \cdots$	Number of un-ionized, first ionized, second ionized, etc., species per unit volume

N_e	Number of electrons per unit volume
N_i	Number of ions per unit volume
N_n	The number of atoms per unit volume in quantum energy state, n
$N_{n'}$	The number of atoms per unit volume in quantum energy state, n′
N_r, N_{r+1}	Particles per unit volume of the species, r and r + 1, respectively
$N_{r,n}$	Particles per unit volume of the species, r, in quantum state, n
n	The n^{th} quantum state
n′	The final total quantum number after a bound-bound or free-bound transition
$Q_{bb}(\nu_{nn'})$	The number of transitions per unit time per unit volume from energy state, n, to lower energy state, n′, producing photons having frequency, ν
$Q_{fb}(\nu)$	Total number of free-bound transitions to all bound quantum levels per unit volume per unit time producing photons having frequency, ν
$Q_{fb}(\nu, n')$	The number of free-bound transitions to quantum energy level, n′, per unit volume per unit time producing photons having frequency, ν
$Q_{ff}(\nu)$	Total number of free-free transitions per unit volume per unit time producing photons having frequency, ν
R	Geometry variable in the axisymmetric jet, illustrated in Fig. 9
r	Geometry variable in the axisymmetric jet, illustrated in Fig. 9
T	Temperature
T_e	Electron temperature
T_{em}	Temperature at which maximum calculated intensity of continuum radiation occurs
T_o	Temperature of the un-ionized species
T_{om}	Temperature at which maximum calculated intensity of a particular spectral line occurs

T_r	Temperature of the species, r
U_o	Electronic partition function of the un-ionized species
U_r, U_{r+1}	Electronic partition function of the r and r + 1 species, respectively
V_r	Ionization potential for the r^{th} state of ionization
v	Velocity
x	Geometry variable in the axisymmetric jet, illustrated in Fig. 9
Y	Geometry variable in the axisymmetric jet, illustrated in Fig. 9
y	Geometry variable in the axisymmetric jet, illustrated in Fig. 9
Z	Effective nuclear charge number
z	Distance from orifice exit to plane of measurement
ϵ	Electric charge of the electron
ν	Frequency of emitted radiation
$\nu_{nn'}$	The frequency of radiation produced by the transition from energy state n to lower energy state n′
$\nu_{n'}$	Frequency of the series limit of bound-bound transitions to energy level n′
ρ	Mass density

INTRODUCTION

Knowledge of the effects of real gas interactions such as dissociation and ionization upon propulsive device performance in the regions of pressure and temperature associated with high-speed flight is presently limited. Although investigations are becoming more numerous, a relatively minor amount of experimental data has been published. A program to obtain such data is underway in the Rocket Test Facility (RTF), Arnold Engineering Development Center (AEDC), Air Force Systems Command (AFSC). The project was designed to produce information which could be used in establishing criteria for the design of nozzles to be used to give ideal expansion in high temperature reacting flows. Three principal areas of investigation were planned: (1) the development of a high temperature gas source which would provide the desired degree of dissociation and ionization, (2) the development of measurement techniques for determining the real state of the gas, and (3) the determination of recombination rates of ionized and dissociated gases. Development of the high temperature gas source has been completed (Ref. 1), and several reliable arc plasma generators have been built. Investigations related to the development of measurement techniques are presented in this report. Future investigations will be directed toward the measurement of recombination rates.

A general plan was adopted for the development of techniques for measuring the energy state of the high temperature gas stream produced by the d-c arc plasma generator. Preliminary analysis of the spectral emission from the gas stream indicated that the radiation consisted of spectral lines, which could be attributed to the gas, and a background of continuous radiation (Ref. 2). Very few spectral lines emitted by either the argon or the helium plasma were found which could not be identified as argon or helium lines. The decision was therefore made to utilize the visible spectrum for the measurement of the energy state of the gas. Conventional pressure and temperature probe measurements as well as electrical probes such as the Langmuir probe were considered to be impractical because of interaction with the gas stream. The probes would necessarily have been water cooled and therefore large compared with the size of the plasma stream. Other diagnostic tools such as microwave apparatus, X-ray apparatus, mass spectrometers, and sonic analyzers were also considered for measurement of the state of the gas, but it was concluded that spectral analysis in the visible portion of the electromagnetic spectrum offered the best possibility for success.

Manuscript released by authors November 1961.

Early work with arc plasma generators (Refs. 3, 4, and 5) indicated that the plasma flame exiting from the orifice electrode consisted (at atmospheric or higher pressure) of a neutral plasma in a state of thermal equilibrium. On this basis, if the temperature could be determined at every point in the stream and if the contamination could be shown to be small, the species concentration, the conductivity (and all other transport properties), the thermodynamic properties, and all other parameters related to temperature could be determined. In addition, if the velocity could also be measured, the recombination rates could be found using the species concentrations determined from temperature distributions. The program that was embarked upon was based on this line of reasoning.

The first step in determining the real state of the gas was the development of a spectrometric method for the measurement of temperature at any point in the atmospheric plasma stream. The approach was to simplify the experimental apparatus as much as possible. Monatomic gases were used for development of the measuring techniques, and operating points of the plasma source were chosen to minimize difficulties resulting from the apparatus itself. The gas most used was argon, although helium was also used on occasion. The spectrometer apparatus was of the conventional type.

This report describes the spectrometric method employed to measure temperature and gives some of the detailed calculations required. Results of these temperature measurements are presented, and the validity of the measurement is evaluated. Finally, some conclusions are drawn relating to the use of the atmospheric plasma jet for gas kinetics research and to modifications which can be made to the jet to render it more useful.

DESCRIPTION OF EXPERIMENTAL APPARATUS

The source of the high energy gas used in the investigations was the direct-current, arc-excited plasma generator facility (Ref. 1) shown in Figs. 1, 2, and 3. A gas, argon in this case, entered the arc chamber tangentially and exited through the orifice electrode (see Fig. 2). The arc was maintained between the tip of the center electrode and the orifice. (Such a configuration of electrodes is generally termed the Gerdien-type configuration.) Energy was added to the gas stream by the interaction of the arc and the constricted flow within the orifice. The orifice electrode was the anode in this case because this connection was found to produce the most stable operation (Ref. 1).

Instrumentation necessary to operate the plasma generator consisted of conventional instruments for indicating and recording gas flow, arc chamber pressure, electric current and voltage, cooling water flow, and cooling water temperature rise (Ref. 1). Data obtained from these instruments were used to construct an energy balance to determine the total power transferred to the gas. The ranges of parameters for normal operation of the generator are shown in Table 1.

Several gases have been used in operation of the plasma generator - helium, nitrogen, argon, air, and mixtures of the inert gases with hydrogen. Argon was selected for the studies reported here because of its availability, because of the stability of the generator when this gas is used, and because a monatomic gas was desired for the ionization studies. Some of the properties of argon which were of use in this study are listed in Table 2.

The axisymmetric plasma flame which exits from the orifice of the generator into the atmosphere radiates a brilliant light immediately downstream of the exit plane and extends about 20 to 25 mm from the 7-mm-diam orifice, spreading slightly as it proceeds downstream. The radiating portion of the jet is illustrated in Fig. 4, which is a photograph taken through a dense, grey filter.

The spectral data in this study were obtained using a Perkin-Elmer 112-U prism instrument equipped with glass optics and a photomultiplier detector. The spectral range of the instrument was 0.2 to 15 micron (only the visible range was used in these experiments), and the data were recorded on a strip-chart recorder. The spectrometer installation is shown in Fig. 1, and its ray path is illustrated in Fig. 5.

Profiles across the entire width of the jet were obtained with the traversing mechanism shown in Fig. 6. The light entered a small collimating aperture and was reflected onto the entrance slit of the spectrometer by a series of mirrors. The plasma generator mount was designed so that the unit could be selectively positioned with respect to the spectrometer to permit traverses at various stations downstream of the nozzle exit plane.

DEVELOPMENT OF A PROCEDURE FOR SPECTROMETRIC MEASUREMENTS

The radiant electromagnetic energy emitted by a high temperature gas is in the form of discrete spectral lines having an intensity somewhat greater than a continuous background radiation spectrum. This

high energy radiation, which heretofore has been available only from the stars and the sun, has been utilized by astrophysicists to determine stellar atmosphere compositions and star temperatures (Ref. 6). The astrophysicists have built up a considerable background of information on methods and applications which can, in large part, be applied to the recently developed high energy gas sources now found in the laboratory.

The literature abounds with information on the theory of quantum physics and atomic structure (Refs. 7 and 8). Also, the formulas relating the radiant intensity of spectral lines and continuum radiation to equilibrium temperature and other atomic and thermodynamic properties are well developed. However, there is a serious lack of data on the various atomic constants to put into these formulas for practical laboratory application. The measurement problem consists, therefore, of the application of the astrophysicists' methods to the radiation from laboratory gas sources and the acquisition of fundamental data on atomic constants.

A number of methods utilizing the theoretical relationships of spectral radiation from the hot gases to the gas temperature have been suggested, and a few have been applied. Other investigators have considered very complicated situations such as an air plasma (Refs. 9 and 10) or have considered the very simple situation such as a direct-current arc in a closed container with an inert gas atmosphere (Ref. 11).

This report is concerned with the diagnosis of the direct-current, arc-excited argon plasma jet. It includes the development of a laboratory method to measure temperature by application of known theoretical relationships to spectrometric measurements of the spectral radiation if an equilibrium temperature can be shown to exist. The species concentrations (neutral atoms, ions, and electrons) can be determined from the measured temperature as functions of the jet geometry. A simple monatomic gas was used to avoid the complications of polyatomic gases and molecular reactions.

THEORETICAL RELATIONSHIPS FOR SPECTRAL EMISSION

The radiant energy emitted from monatomic plasmas results from transitions of bound electrons from higher to lower quantum states (discrete spectral lines) and from transitions of free electrons either to bound states (recombination) or to free states (Bremmsstrahlung) of lower energy. Transitions of free electrons produce continuum radiation because the energy of the free electron is not quantized. In fact, if the gas is in equilibrium, the electrons will have a continuous, Maxwellian distribution of energy.

Spectral Line Radiation

The transitions giving rise to spectral lines are referred to here as bound-bound transitions. The number of such transitions per unit volume per unit time accompanied by radiation at the discrete frequency, $\nu_{nn'}$, is (Refs. 6 and 7):

$$Q_{bb}(\nu_{nn'}) = A_{nn'}N_n + B_{nn'}N_nD(\nu_{nn'}) - B_{n'n}N_{n'}D(\nu_{nn'}) \quad (1)$$

where the three components are the spontaneous emissions, the induced emissions, and the induced absorptions, respectively. The three transition probabilities are related as follows (Ref. 6):

$$A_{nn'} = \frac{8\pi h \nu_{nn'}^3}{c^3} B_{nn'}$$

$$g_n B_{nn'} = g_{n'} B_{n'n}$$

Assumption of Equilibrium

If a Maxwellian distribution of the energies of the particles in a system exists, then the system is in a state of thermodynamic equilibrium, and a temperature can be defined. In a plasma containing neutral atoms, electrons, and ions in one or more degrees of ionization, equilibrium implies that there exists a single Maxwellian distribution of the velocities of each particle species and that a single temperature exists. Furthermore, the excited states of the neutral atoms or ions will be distributed according to the Boltzmann formula (Ref. 12):

$$N_{r,n} = \frac{N_r g_{r,n}}{U_r} \exp\left[-\frac{E_{r,n}}{kT_r}\right] \quad (2)$$

where the subscript r denotes the r species. The atomic excitation temperature T_r in Eq. (2) was designated with the r species subscript to illustrate the possibility of measuring the excitation temperature of each species separately. If the temperatures of the different species turn out to be the same, then equilibrium must exist.

Another result of the equilibrium assumption is that, for a monatomic gas, the number densities of the neutral atoms, the electrons, and the various ionic species can be expressed by the general equation:

$$\frac{N_{r+1}N_e}{N_r} = \left[\frac{\sqrt{2\pi m_e k}}{h}\right]^3 \frac{2U_{r+1}}{U_r} T^{3/2} \exp\left(-\frac{V_r}{kT}\right) \quad (3)$$

This is the generalized Saha equation of ionization (Ref. 13). The temperature T in this equation is the thermal temperature of the gas.

Continuum Radiation

In a thermally ionized gas, the free electrons are bounding about with a continuous, Maxwellian velocity and energy distribution. Thus, if an electron enters the electric field of an ion, it will either be captured or its path will be altered by the influence of the field. If it is captured, the recombination results in the transition of the free electron to a bound quantum state accompanied by the emission of a photon of radiation. Since the distribution of energy of the electrons before recombination is continuous, the radiant energy emitted will be continuous with frequency ν. A quantitative accounting for such transitions of free electrons has been calculated accurately only for a hydrogen gas. However, the general form of the equations would be the same for more complicated atoms. The number of such free-bound transitions to quantum level n' per unit time per unit volume accompanied by radiation at frequency ν is (Refs. 12 and 14):

$$Q_{fb}(\nu, n') = K \frac{4\pi^2 \epsilon^4 m_e}{h^2 n'^3} \cdot \frac{1}{h\nu} \cdot Z^4 \frac{N_e N_i}{(kT_e)^{3/2}} \exp\left[\frac{h}{kT_e}(\nu_{n'} - \nu)\right] \tag{4}$$

where

$$K = \frac{32\pi^2 \epsilon^6}{3\sqrt{3}\, c^3 (2\pi m_e)^{3/2}}$$

and T_e is the electron temperature. At a given frequency ν the total number of photons resulting from free-bound transitions is the sum of the transitions to all quantum levels:

$$Q_{fb}(\nu) = \sum_{n'} Q_{fb}(\nu, n') \tag{5}$$

If the electron is not captured by the ion, its energy will be altered to a lower state, again with a transition giving rise to radiant emission continuous with frequency ν. The number of free-free transitions giving rise to radiation at frequency ν is (Refs. 12 and 14):

$$Q_{ff}(\nu) = K \cdot \frac{1}{h\nu} \cdot Z^2 \frac{N_e N_i}{(kT_e)^{1/2}} \exp\left(-\frac{h\nu}{kT_e}\right) \tag{6}$$

where K is the same constant used in Eq. (4).

DEVELOPMENT OF THE EXPERIMENTAL METHOD

Intensity Relationships

The expressions for the spectral line and continuum radiation have been applied in many ways to the problem of measuring the temperature

of high energy gases (Ref. 12). Initially, a great deal of effort was applied at AEDC to making temperature measurement by the distribution of the intensities of several spectral lines. These efforts proved fruitless because of difficulties in obtaining transition probability data and an intensity calibration of the spectrometer. Attempts were also made to measure temperature by Doppler shifts and collision broadening, but these efforts failed because of the insufficient resolution capabilities of the available spectrometer equipment. The general "peaking function" method used in the present work for the measurement of temperature has been used in other applications (Refs. 11 and 15). The method avoids many of the difficulties resulting from (1) the experimental error encountered in making absolute measurements or (2) in the calibration of intensity as a function of wavelength, and it does not require knowledge of the transition probabilities. However, the application and methods presented here are sufficiently different from those noted in the published literature to warrant a complete description.

Spectral Line Intensity. The intensity of a particular spectral line of frequency, $\nu_{nn'}$, emitted from the neutral atoms of a gas in thermal equilibrium can be expressed as

$$I_{bb}(\nu_{nn'}) \propto \left(\frac{N_o}{U_o}\right) \exp\left(-\frac{E_{o,n}}{kT_o}\right) \tag{7}$$

This relationship results if the induced terms in Eq. (1) are neglected and Eqs. (1) and (2) are combined. [The intensity quantity I used in this section, Eqs. (7), (10), and (12), is related to the quantity Q of the previous section, Eqs. (1), (4), and (6), by $I \propto h\nu Q$.] The first part of Eq. (7), N_o/U_o, decreases monotonically from a finite value at low temperature toward zero at high temperature, since N_o decreases with increasing temperature because of the decreasing density and also because of increased ionization and since U_o increases with temperature. The second term of Eq. (7) increases monotonically from zero at zero temperature and approaches unity at high temperatures. Because the product of these two functions is zero for small values of T and zero for large values of T but finite in between and because the functions are monotonic, the intensity must reach a maximum at some temperature, T_{om}. Thus, if the temperature at the maximum intensity condition can be calculated, this point will serve as a calibration point upon which to base the measurements.

Because all the terms in Eq. (7) are calculable, the product function can be determined. Thus, N_o can be determined by use of the equation of state for a perfect gas and the Saha equation, Eq. (3), and the atomic partition function, U_o, can be expressed as

$$U_o = \sum_n g_{o,n} \exp\left(-\frac{E_{o,n}}{kT}\right) \tag{8}$$

The method of calculating the partition functions and the particle densities is discussed in Appendixes A and B, respectively. Values of N_o for argon are shown as a function of temperature in the graph in Fig. B1, which also contains all appreciable ion concentrations and the electron concentration. The variation of U_o with temperature for argon is shown in Fig. A1.

The 4158 Å line of neutral argon was chosen for the present study because of its prominence and clarity in the spectrum. The transition for the 4158 Å line is $3p^5 4s\,[1\,1/2]^\circ - 3p^5 5p\,[1\,1/2]$ where the notation is that of Ref. 16, and the corresponding energy above the ground level is 117,183 cm^{-1} (cm^{-1} x 4.75 x 10^{-24} = cal). The normalized peaking function, Eq. (7), for the 4158 Å line is given in Fig. 7. Note that the maximum occurs at a temperature of 15,500°K. Any other visible spectral line of neutral argon will exhibit a maximum intensity very near 15,000°K since $E_{o,n}$ ranges only from about 112,000 to 127,000 cm^{-1}.

The experimental procedure is thus reduced to a relatively simple measurement. If a plasma exists in which the excitation temperature at the center is greater than the reference temperature, T_{om}, then the instrumentation problem is to find the position in the plasma where $T = T_{om}$ and to normalize all intensity readings to the intensity at this value of temperature. The means of accomplishing this will be described in a subsequent section.

Continuum Radiation Intensity. The continuum intensity relationships, Eqs. (4) and (6), also exhibit peaking characteristics so that the electron temperature can be determined in a manner similar to the method used to determine the atomic excitation temperature. The free-bound transitions will contribute continuum intensity at a frequency, ν, according to Eqs. (4) and (5). At a wavelength of 4150 Å, the free-bound radiation from an argon plasma corresponds to transitions having energy changes greater than 24,100 cm^{-1} so that the principal bound state is $3p^5 4p$, which has a minimum level of 104,100 cm^{-1} and a maximum level of 108,700 cm^{-1} with a multiplicity of levels between. Assuming that most of the radiation at 4150 Å is the result of transitions to $n' = 4$ (note that the summation in Eq. (4) decreases as $1/(n')$) and taking 106,400 cm^{-1} as the average level to which the electron falls, the intensity of the free-bound continuum radiation at 4150 Å is [see Eq. (4)]:

$$I_{fb}(\nu) = 2.68 \times 10^{-35} \left[\frac{N_e N_i}{T^{3/2}} Z^4\right]\left[\exp -\left(\frac{4850}{T}\right)\right] \qquad (9)$$

where the energy units are relative.

The contribution to the continuum intensity from an argon plasma at 4150 Å by free-free transitions is given by Eq. (6) and can be expressed numerically as follows:

$$I_{ff}(\nu) = 5.44 \times 10^{-39} \left[\frac{N_e N_i}{T^{1/2}} Z^2\right]\left[\exp\left(-\frac{36000}{T}\right)\right] \tag{10}$$

Again, the energy units are relative and are the same as for Eq. (9).

The ion and electron densities for argon can be found in Appendix B, and the effective nuclear charge is given by

$$Z = \frac{N_o + 2N_1 + 3N_2 + \cdots}{N_o + N_1 + N_2 + \cdots} \tag{11}$$

Therefore, the functions can be calculated over the temperature range 0 to 50,000°K.

The total continuum intensity is given by the sum of the free-bound and free-free contributions. All three functions - free-bound, free-free, and their sum - are shown plotted on a relative basis in Fig. 8, where the normalization was taken at the first maximum of the sum relationship. The resulting peaking function makes possible the determination of electron temperature in much the same way as the excitation temperature can be determined from Fig. 7.

It should be noted that at the temperatures considered here, the major contribution to the continuum intensity results from recombination transitions. This would not necessarily be true for higher temperatures and lower gas densities, and such cases would need to be investigated individually.

Geometry Problem of the Axisymmetric Source

In an axisymmetric gas stream the density dependent properties such as light intensity emission or absorption are necessarily functions of the radius. However, measurement of such properties can only be made from the outside, as illustrated in Fig. 9. Such a measurement, denoted as F(x) in the figure, is a result of all the elements of I(r) dy along the measurement path, that is:

$$F(x) = \int_{-Y}^{+Y} I(r)\, dy \tag{12}$$

At fixed values of x, $y^2 = (r^2 - x^2)$ and $dy = r(r^2 - x^2)^{-1/2} dr$, and Eq. (12)

becomes

$$F(x) = 2\int_{x}^{R} \frac{r\,I(r)}{\sqrt{r^2 - x^2}}\,dr \tag{13}$$

where the limits are modified accordingly.

The measurement of the spectral intensity obtained at different points along the x-axis using the traversing mechanism shown in Fig. 6 results in a lateral profile, $F(x)$. The measurement of interest, however, is $I(r)$ which can be obtained (Ref. 17) by inversion of Eq. (13) to the form:

$$I(r) = -\frac{1}{\pi}\int_{r}^{R} \frac{F'(x)}{\sqrt{x^2 - r^2}} \tag{14}$$

where $F'(x)$ is the derivative of $F(x)$ with respect to x. Then, if an experimental distribution, $F(x)$, is known, the derivative can be calculated, and the integral can be evaluated numerically to give $I(r)$. It is this $I(r)$ which must be used to determine a temperature from the calibration curves shown in Figs. 7 and 8.

Experimental Procedure

The procedure used in the experiments may be simply stated as follows:

1. After the arc jet was started and allowed to stabilize, the data for an energy balance were recorded.
2. The traversing mechanism was then used to obtain lateral profiles of both continuum and line intensity at a given plane along the jet axis. The procedure consisted of setting different positions across the jet and scanning over about a 20-Å range so that the complete spectrum line was obtained at each position. The continuous radiation on the short wavelength side (4150 Å) was used for the continuum radiation profiles. Continuum profiles were also obtained by a continuous traverse across the jet with the spectrometer set at a constant wavelength.
3. The plasma generator was moved along its longitudinal axis, and procedure 2 was repeated to obtain intensity profiles at different planes along the jet axis.
4. The lateral profiles so obtained were plotted and normalized and then numerically inverted to radial profiles by a direct solution of Eq. (14) using an IBM-7070 digital computer. The radial profiles were also normalized and plotted, and from these curves the temperature measurement was made by cross reference between the radial profiles and the peaking functions.

RESULTS AND DISCUSSION

DATA OBTAINED FROM ARGON PLASMA

Data were obtained, using the procedure described, for many different operating conditions of the plasma generator using argon. Four sets of data are presented in this report to demonstrate repeatability, to show the dependence of the temperature with enthalpy and orifice material, and to demonstrate that self-absorption can be neglected. The four sets of data are given in Figs. 10 through 13; the data in Figs. 10, 11, and 12 differ only in the operating conditions of the plasma generator. The operating data are given in Table 3.

Consider first Fig. 10a, an example of the method of temperature determination. Shown in this figure are the experimentally determined lateral intensity profiles for both the spectral line emission (4158 Å) and continuum emission (~ 4150 Å) after normalization, the inverted radial intensity distributions (also normalized), and the temperature profiles which result from a cross plot of the radial distributions and the peaking functions.

The most notable attribute of both the spectrum line and the continuous intensity radial profiles is the off-center peaking. If temperature is assumed to be a monotonic function of the radius with a maximum temperature occurring at the center of the stream (and this seems to be the only plausible assumption), then the off-center peaks must be associated with the peaking function curves (Figs. 7 and 8), and the temperature at the point in the stream where the maximum intensity occurs must be T_{om}. Thus the values of I(r) to the left of the peaks in Fig. 10a must correspond to values of temperature to the right of the maximum on the peaking function curves (temperatures greater than T_{om}), and values of I(r) to the right of the peak must correspond to values of temperature less than T_{om}. Radial profiles of the excitation temperature were determined from a cross plot of Fig. 7, the spectral line peaking function, and the radial distribution of line intensity; the temperature plot is shown at the bottom of Fig. 10a.

The continuum intensity profiles were very similar to those obtained for the line intensity and also had one off-center peak. Thus, the temperature determination procedure was very much the same except that the peaking function of Fig. 8 was used. The electron temperature profile determined from the continuum intensity data is also shown in Fig. 10.

When the excitation temperature profile was compared with the electron temperature profile, it was found that the two temperatures deviated

by no more than 10 percent at the jet center and by no more than 2 percent over most of the profile.

Data for various planes of measurement and power levels of the plasma generator are shown plotted in the same manner in Figs. 10b, 11a, 11b, 12a, and 12b as was shown in Fig. 10a, and the same reasoning was used to obtain the temperature profiles. Figures 10a and b were obtained for the same jet at two planes along the axis, Fig. 10a at a distance 6 mm from the orifice exit and Fig. 10b at a plane 19 mm from the orifice exit. The temperature obtained for the downstream plane (z = 19 mm) was slightly less all across the profile than the temperature at the z = 6-mm plane. Also, it can be seen that the temperature obtained using the spectral line data agrees more closely with that obtained using the continuum emission data for the downstream plane. This is perhaps an indication of a closer approach to equilibrium between electrons and excited atoms at the downstream plane.

The data shown in Fig. 11 were taken at nearly the same generator operating conditions but at a different time and using a copper orifice electrode instead of a carbon electrode. The data are not significantly different from those in Fig. 10. The data shown in Fig. 12 were taken at about one-half the power level used for the data in Figs. 10 and 11. However, it can be seen that the resulting temperature profiles are, again, not very different from those obtained using higher power levels. The reason for this apparent discrepancy will become clear in the discussions to follow. (The reason for the deviation shown between excitation and electron temperature in Fig. 12b at the extremity of the jet is not known.)

SELF-ABSORPTION

The possibility that self-absorption influenced the measurements was also explored. The data presented in Fig. 13 were taken to show the effect of the self-absorption. For this measurement a plane mirror was placed above the plasma flame (Fig. 6) and adjusted until a light passing from the spectrometer through the collimating aperture was exactly reflected back through the aperture. Spectral data were then obtained with the mirror covered and with it uncovered; the data for the spectral line are shown in Fig. 13a and for the continuum emission, in Fig. 13b. In these plots, the experimental measurement (normalized at the maximum of the data taken with the mirror uncovered) is shown at the top. The radial profiles are shown in the center and were normalized at the off-center peaks. The temperature is shown at the bottom of the graphs and was obtained by the method used to obtain the temperature profiles

shown in Fig. 10a. The significance of these results is that no evidence of self-absorption could be detected because practically the same temperature profiles were obtained with and without the mirror.

DISCUSSION OF THE MEASUREMENT OF ARGON PLASMA TEMPERATURE

The agreement between the excitation temperature of the neutral argon atom and the temperature of the recombining electrons demonstrated by the data presented leads to the belief that the two processes which gave rise to the spectral line and continuous radiation were near equilibrium. Thus it appears that the distribution of the excited states of the neutral argon atoms was very nearly Maxwellian and also that the velocities of the free electrons were distributed in a Maxwellian fashion. The fact that two of the possible distributions of energy within the gas appeared to be equilibrium distributions is an indication that the remaining energies, such as translation energy, might also be distributed according to the equilibrium law and that the different forms of activity might be in equilibrium with each other. The measured value of temperature would then be the thermal temperature of the gas.

At equilibrium the distribution of neutral and ionic species is given by the Saha equations which were used to determine the species concentrations (Appendix B). Figure 14 is the result of a cross plot of the electron temperature profiles (Figs. 10a and b) and the species concentrations (Fig. B1) to give particle density profiles of the jet at the two positions of measurement. Note that if the velocity of the jet between the two positions along the axis were known, it would be possible to determine recombination rates of the electrons and ions.

APPLICATION TO HELIUM PLASMA

Experiments similar to those described above were made using helium as the working gas. The maxima for the helium peaking functions occur at about 25,000°K. When the radial inversion was made on the lateral profiles obtained from the helium jet, the off-center maximum did not occur. It was concluded that the temperature at the jet center was less than 25,000°K and that thus the calibration point could not be defined. The peaking function method could not be used for the helium plasma for this reason.

EVALUATION OF THE MEASUREMENT

TEMPERATURE COMPARISON

The problem remains of interpreting the measurement of the temperature profile of the argon jet in the light of other known data. The first discrepancy in the temperature measured by the spectrometric method was found in the comparison of the temperature profiles in Figs. 11 and 12. Although the power to the gas differed by a factor of two, the measured temperature profiles were practically identical. Another discrepancy appeared when the average temperature from the spectrometric data was compared with the average temperature determined from an energy balance. Figure 15 is a plot of temperature vs specific enthalpy of the gas as determined from an energy balance over a large range of plasma generator operating conditions (Ref. 1). From Table 3 the specific enthalpy for the data in Fig. 10 determined from the energy balance is 630 cal/gm, which corresponds to an average temperature of 5000°K from the caloric equation of state or 3200°K from the equation of flow through an orifice of a perfect gas (Ref. 1). Comparison of these values with the average temperature shown in Fig. 10a reveals that the temperature determined by the spectrometric method is larger by a factor of three or more. Clearly, then, the spectrometric measurement must be examined more thoroughly.

ENTHALPY COMPARISON

Temperature alone is not a sufficient parameter for comparison because of the distribution of the energy in an ionized gas into the various ionization and excitation states, as well as translational energy, and also because of the density distribution across the stream. It would seem logical to compare the total enthalpy determined from the spectral data with that obtained from the energy balance. The specific enthalpy, specific heats, and species concentrations of a gas at a given pressure can be calculated as functions of temperature (Ref. 18). This calculation, however, is a very tedious one because of the summation of states and electronic energy over a large number of quantum states. The fundamentals of the calculation are given in Appendix C, and the specific enthalpy of the argon species is given as a function of temperature in Fig. C-2. These calculations were made using a large digital computer, and the results were used to determine the total stream enthalpy from the temperature as measured using the spectrometric method.

To determine total enthalpy, the integral $\int_0^A \rho v h^* dA$ must be evaluated, where ρ is the mass density, v is velocity, h^* is the specific enthalpy, and dA is the elemental area. Now ρ, the particle density, and h^* for any temperature were known as functions of the radius, r, so that $\rho(r)$ and $h^*(r)$ could be determined. However, the velocity distribution was unknown, and resort was made to an assumption of the dependence of $v(r)$. It was assumed that the Mach number was constant across the stream so that $v \propto \sqrt{T}$, and since $(\rho v)_{avg}$ was known from the gas total mass flow, a scale for the (ρv) distribution could be determined. In this way $\rho v(r)$ as as a single function was found, and the integral $\int_0^R (\rho v) h^* (2\pi r dr)$ was evaluated. The procedure is illustrated in Fig. 16, and the numerical values are shown for the data presented in Fig. 10a. The final answer was obtained from the area under the curve of $\rho v h^*$ vs πr^2, which gave 7, 225 cal/sec as the total energy of the gas stream.

Comparison of the spectrometrically determined enthalpy with that from the energy balance (2390 cal/sec) clearly shows that the temperature determined from the spectrometric data must not be the average temperature of the gas. It is apparent that a similar treatment of the data of Figs. 11 or 12 would yield the same relative result. The physical situation must therefore be re-examined to seek an explanation for this discrepancy.

JET STRUCTURE

Many explanations of the energy transfer mechanism within a Gerdien-type arc plasma generator have been presented (Ref. 19). Most of these assume that the arc or electron current path is maintained within the arc chamber or orifice electrode as shown in Fig. 17a. However, if the current paths were to extend beyond the orifice and were in some way to return to the positive electrode, as suggested by Fig. 17b, then a great deal of collisional activity would be occurring in certain portions of the jet, while the remainder of the jet would not be disturbed at a particular time. This erroneous spectrometric temperature measurement might be explained because most of the radiation would be produced in the high energy arc channels. A detailed investigation of the electrical structure of the jet was made and is reported in Ref. 20.

The first attempts to study the possibility of arc paths outside the orifice consisted of taking very high speed photographs ($\approx$ 500, 000 frames per second) of the jet in an effort to define a single arc channel, which was assumed to be moving around at random at high frequency. No such

definition of an arc channel could be obtained, even on pictures taken at near 600,000 frames per second using a drum-framing camera. The conclusion from these results was that if the current paths did exist, they were not defined in narrow channels or else were occurring at a very high frequency.

A second method of study utilized various electrical probes which were inserted into the stream. The most significant result was obtained by inserting a length of 1/4-in. -diam tungsten into the stream in an effort to split the current between the positive electrode and the probe by providing a lower resistance path for the current flow. The electrical schematic is shown in Fig. 18. It was found that approximately 10 percent of the total current could be drawn through the probe path when the probe was very near the orifice exit and that as much as 5 percent could be drawn near the tip of the intense cone (19 mm). The three currents - probe, negative electrode, and positive electrode - were measured by shunts and millivolt bridges. When the probe was inserted, the current through meter 2 decreased by just the amount of increase of meter 1 while the total current through meter 3 did not change. This experiment offered positive indication of the existence of current paths downstream of the orifice.

Other types of probes were also used to add to the information concerning the atmospheric jet. A double probe (Ref. 20) was used to show a reversal in polarity of the potential as the probe was inserted into the stream. This result indicated a loop structure such as hypothesized in Fig. 17b. A Langmuir probe study showed the departure from equilibrium of the electron velocity as the probe was inserted deeper into the stream. Several other studies which support the extended arc hypothesis are described in detail in Ref. 20.

EVALUATION OF TEMPERATURE MEASUREMENT

A plausible explanation can now be made for the disagreement between the spectrometric and energy balance measurement of temperature. The spectrometric method of temperature measurement presented is valid. Also, it has been established that electric arcs exhibit equilibrium behavior and that a temperature can be ascribed to an arc. The difference is that the luminous gas stream to which the spectrometric method is being applied consists partly of an undisturbed hot gas and partly of an electric arc at any one instant of time. The electrons and gas atoms within the current path are emitting freely and are at essentially the electron temperature. However, the gas atoms that are not within this small high energy path are at much lower temperature and are not emitting

appreciable radiation. The apparent temperature measured spectrometrically is thus a correct measurement for the freely emitting species, but it is only applicable to a small portion of the gas stream and does not represent an average temperature of the entire gas jet.

EVALUATION OF THE ATMOSPHERIC PLASMA JET FOR GAS KINETICS RESEARCH

The hot gas jet produced by the Gerdien-type d-c arc plasma generator used here is not adequate for gas kinetics research because the jet consists of an extended arc in a state of instability through which the gas flows. A single temperature cannot be ascribed to this jet, and a non-equilibrium state exists. The temperature measured by the spectrometric method seems to be a valid measurement of the electron temperature within the arc but is not the gas temperature. The problem then is to determine whether some other configuration of the generator can provide the characteristics required of the gas source.

One solution to the problem would be to contain the arc within the arc chamber of the plasma generator by a suitable design of electrodes. Many designs of electrode configurations have been made which effectively contain the arc (Ref. 19). None of these are of the Gerdien type. However, the possibility of non-uniform heating would need to be investigated. Data have not been published to show the uniformity of the hot jets produced by the various configurations.

Another possible solution would be to provide a plenum chamber between the orifice electrode and an exit nozzle. Such a plenum was tested at AEDC. A large amount of energy was lost to the walls of the plenum chamber, and the intensity of the exit jet was not sufficient to allow spectrometric measurements.

A third method which might provide a suitable gas source for use in studying the kinetics of high temperature gas flows is that of expanding the jet into a low pressure region and utilizing the expanded stream. Such a low pressure test cell has been built (Fig. 19), and a plasma generator has been exhausted into low pressures on the order of 0.2 to 2 mm Hg. The expanded plasma flame shown in Fig. 20 illustrates the region which could be used for the kinetics measurements.

The electrical probe measurements made for the atmospheric jet were repeated for the expanded stream (Ref. 20). The results showed that the blown arc region is contained within the small hot core near the orifice but is not blown downstream more than about 25 mm. Furthermore,

Langmuir probe measurements showed that the electron velocity distribution in the expanded jet was essentially Maxwellian and that electron temperatures were on the order of 4000 to 8000°K. It was concluded that the expanded arc jet should provide a satisfactory high energy gas source for gas kinetics measurements.

The peaking function method of temperature measurement used for the atmospheric argon jet depends upon the existence of a temperature, at some place in the jet, in excess of 16,000°K. These criteria were satisfied in the atmospheric jet because of the high electron temperatures. However, at low pressures the temperature of the expanded jet is much less than 16,000°K, and the peaking function method is not applicable. Thus, new spectrometric methods must be developed for measuring the temperature of the expanded jet.

CONCLUSIONS

The d-c arc plasma generator using the Gerdien-type electrode configuration provides a useful hot gas radiating source for use in developing spectrometric measurement techniques. The "peaking function" spectrometric method of measuring the temperature of the hot gas source was found to be a very useful and convenient tool, provided temperatures in excess of the calibration temperature existed in the jet (16,000°K for argon); the range of measurement was then from 7000 to 28,000°K for argon plasma.

The temperature measured at the center of the argon plasma jet exhausting to atmospheric pressure was found to be approximately 18,000°K when the spectrometric measurement method was used. The measurements were found to be repeatable, and it was shown that self-absorption could be neglected. The temperature measured from spectral line intensities was found to agree very well with measurements obtained using the continuum intensity. However, it was shown that the temperature in both cases was actually the electron temperature rather than the average gas temperature. Furthermore, it was shown that the atmospheric jet contained blown arc paths which were responsible for the high temperature measurement; the actual average gas temperature was found by an energy balance to be less than the temperature determined by the spectrometric method by a factor as high as three.

Values of the electronic partition function, the thermodynamic properties, and the species concentrations of argon and helium over the temperature range from 5000 to 50,000°K were calculated during these studies.

These data will be quite useful for any studies involving argon and helium gas at high temperature.

It was concluded that the atmospheric jet from the Gerdien-type generator cannot be used as a gas kinetics research tool because of the complexity of the electrical structure in the jet. However, at low pressures the expanded portion of the jet produced by the same electrode configuration was found to be free of such current paths and should provide an adequate hot gas source.

REFERENCES

1. McGregor, W. K., Ehrlich, J. J., and Dooley, M. T. "Performance of a D-C Arc-Excited Plasma Generator." AEDC-TN-60-112, August 1960.
2. McGregor, W. K., Ehrlich, J. J., and Bratcher, J. D. "The Visible Plasma Flame Spectra of Argon and Helium." AEDC-TN-59-134, December 1959.
3. Giannini, Gabriel M. "The Plasma Jet." Scientific American, August 1957.
4. Ghai, M. L. "Plasma Generation Facility and Some Research Results." Conference on Extremely High Temperatures. John Wiley & Sons, New York, 1958, p 221.
5. Browning, James A. "Techniques for Producing Plasma Jets." Dynamics of Conducting Gases. Northwestern University Press, 1960, p 126.
6. Aller, Lawerence H. Astrophysics. The Ronald Press Co., New York, 1953.
7. Slater, John C. Quantum Theory of Matter. McGraw-Hill Book Co., New York, 1951.
8. Herzberg, Gerhard. Atomic Spectra and Atomic Structure. Dover Publications, New York, 1944.
9. Pearce, Willard S. "Plasma Jet Temperature Study." WADC TR-59-346, July 1959.
10. Dickerman, P. J. ed. "Experimental Studies of the Temperature in a Field-Free Plasma." Symposium on Optical Spectrometric Measurements of High Temperatures. University of Chicago Press, 1960.

11. Olsen, H. N. "Thermal and Electrical Properties of an Argon Plasma." The Physics of Fluids. November-December 1959.

12. Wulff, H. "Plasma Diagnostics by Spectroscopical Means." Nuclear Instruments and Methods. North Holland Publishing Co., 1959, pp 352-362.

13. Duclos, Donald P. "The Equation of State of an Ionized Gas." AEDC-TN-60-192, October 1960.

14. Finkelnburg, W. and Peters, Th. "Kontinuierliche-Spektren." Handbuch der Physik, Vol. XXVIII, Spectroscopy II. Berlin, 1957.

15. Burhorn, F., Maecker, H., and Peters, T. "Temperature Measurements on Water-Stabilized High-Power Arcs." Translation from Zeitschrift für Physik, Vol. 131, 1951 by Langley Aeronautical Lab, NACA, January 1957.

16. Moore, Charlotte E. Atomic Energy Levels, Vol. 1. National Bureau of Standards Bulletin No. 467, Washington, D. C., 1949.

17. Dooley, M. T. and McGregor, W. K. "Calculation of the Radial Distribution of the Density Dependent Properties in an Axisymmetric Gas Stream." AEDC-TN-60-216, May 1961.

18. Kelley, K. K. "Contributions to the Data on Theoretical Metallurgy; High-Temperature Heat-Content, Heat-Capacity and Entropy Data for Inorganic Substances." Bureau of Mines, Bulletin No. 371, 1933.

19. John, Richard R. and Bade, William L. "Recent Advances in Electric Arc Plasma Generation Technology." ARS Journal, Vol. 31, No. 1, p. 4, January 1961.

20. Dooley, M. T., McGregor, W. K., and Brewer, L. E. "Characteristics of the Arc in a Gerdien-Type Plasma Generator." AEDC-TR-61-13, November 1961.

TABLE 1

NORMAL RANGE OF THE OPERATING VARIABLES FOR THE PLASMA GENERATOR USING ARGON

Voltage	25 - 75 volt
Current	30 - 1000 amp
Power	2 - 60 kw
Gas Flow	1 - 20 gm/sec
Arc Chamber Pressure	1 - 8 atm
Efficiency	60 - 90 percent $\left(\frac{\text{total power - losses}}{\text{total power}}\right)$
Orifice Diameter	4 - 12 mm
Arc Gap	3 - 6 mm
Contamination	less than 0.05% by weight

TABLE 2

PROPERTIES OF ARGON

Atomic Number		18
Atomic Weight		39.96
Density (0°C, 1 atm)		4.784 gm/lit
Ionization Potentials -	First	15.76 volt
	Second	27.62 volt
	Third	40.90 volt
	Fourth	59.8 volt

TABLE 3

OPERATING CONDITIONS OF PLASMA GENERATOR USED WHEN MAKING SPECTROMETRIC MEASUREMENTS

Operating Point	1 Fig. 10	2 Fig. 11	3 Fig. 12	4 Fig. 13
Power - kw	12.50	11.13	5.85	9.03
Gas Flow - gm/sec	3.80	3.20	3.02	4.87
Chamber Pressure - atm	1.83	1.47	1.29	1.81
Efficiency - %	80	61	64	72
Specific Enthalpy - k-cal/kgm	630	510	297	321
Type Orifice Electrode	Carbon	Copper	Copper	Copper
Temperature - °K (Caloric Equation)	5200	4363	2665	2859
Temperature - °K (Flow Equation)	3200	2800	2000	2100

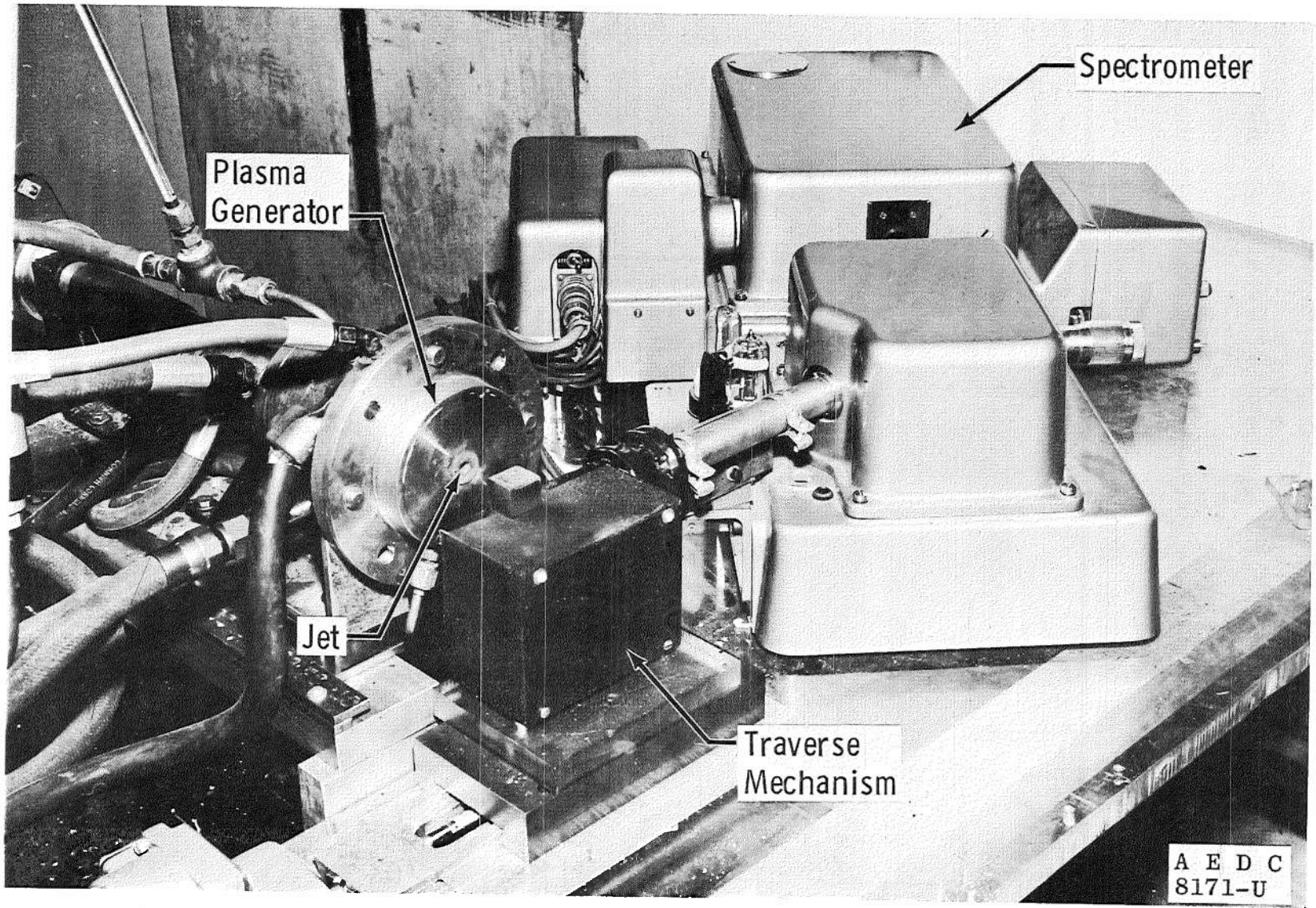

Fig. 1 Photograph of the Plasma Generator and Spectrometer Used for Spectrometric Temperature Measurements

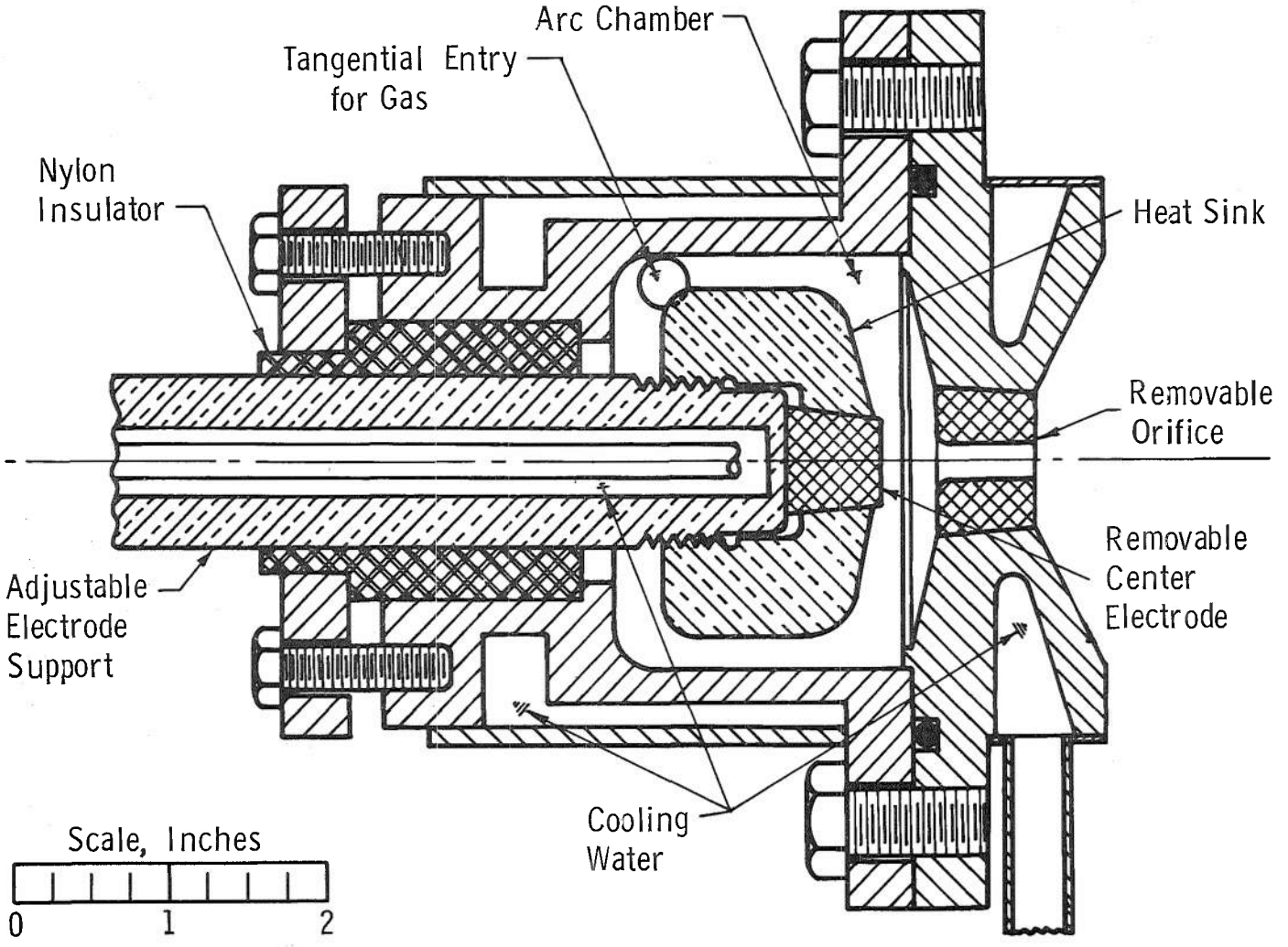

Fig. 2 Cross-Sectional View of the Gerdien-Type Plasma Generator

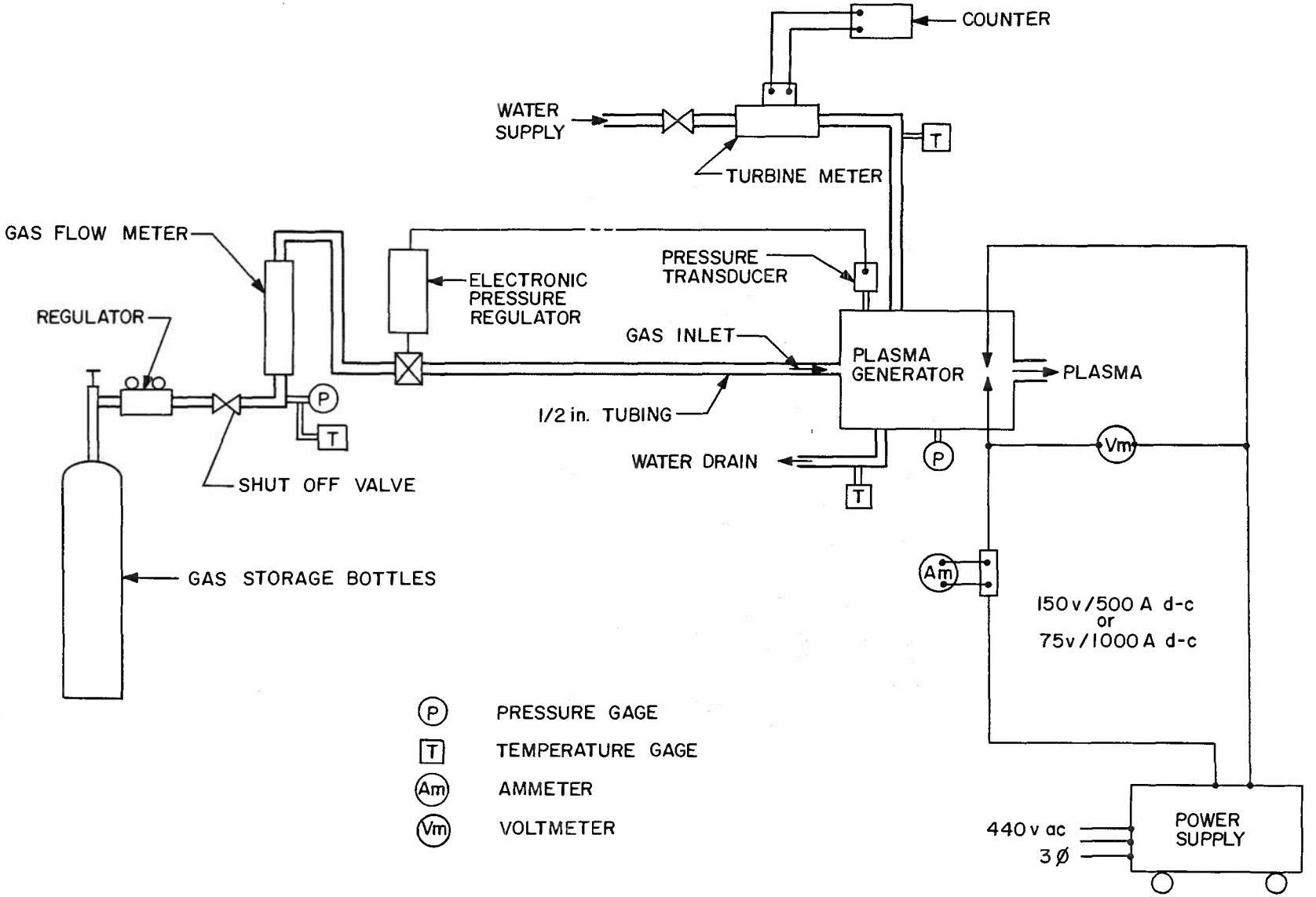

Fig. 3 Flow Diagram of the Plasma Generator Facility Used at AEDC

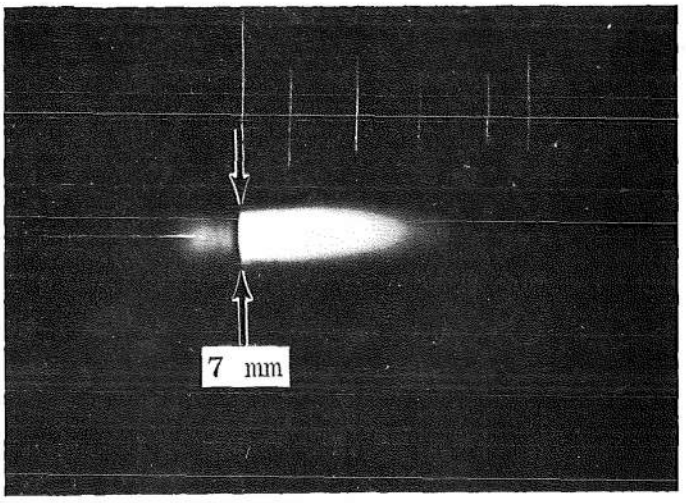

Fig. 4 Photograph of the Plasma Jet Structure Taken through a Dense, Grey Filter

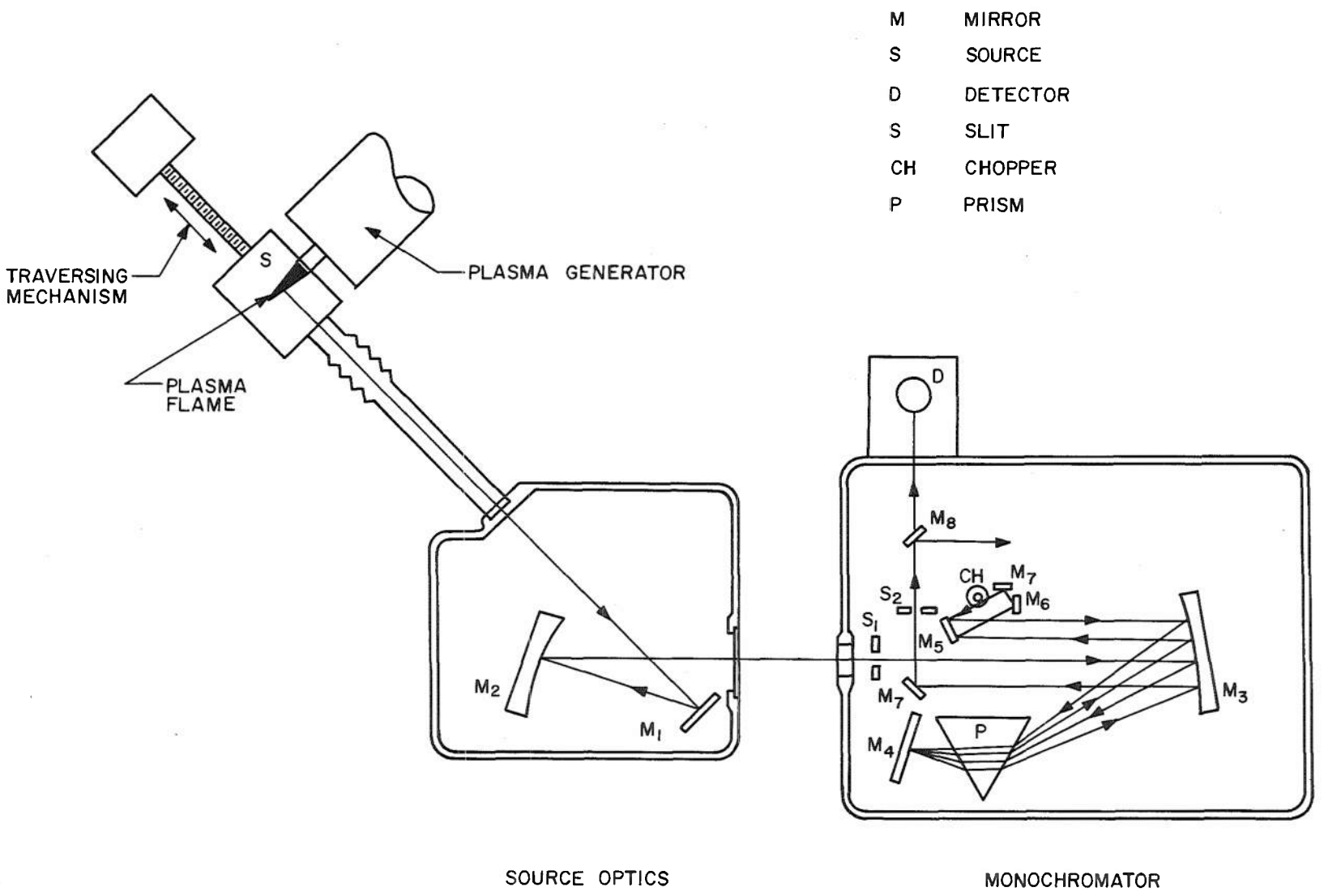

Fig. 5 Plasma Flame and Spectrometer Arrangement for Obtaining Quantitative Spectral Intensity Data

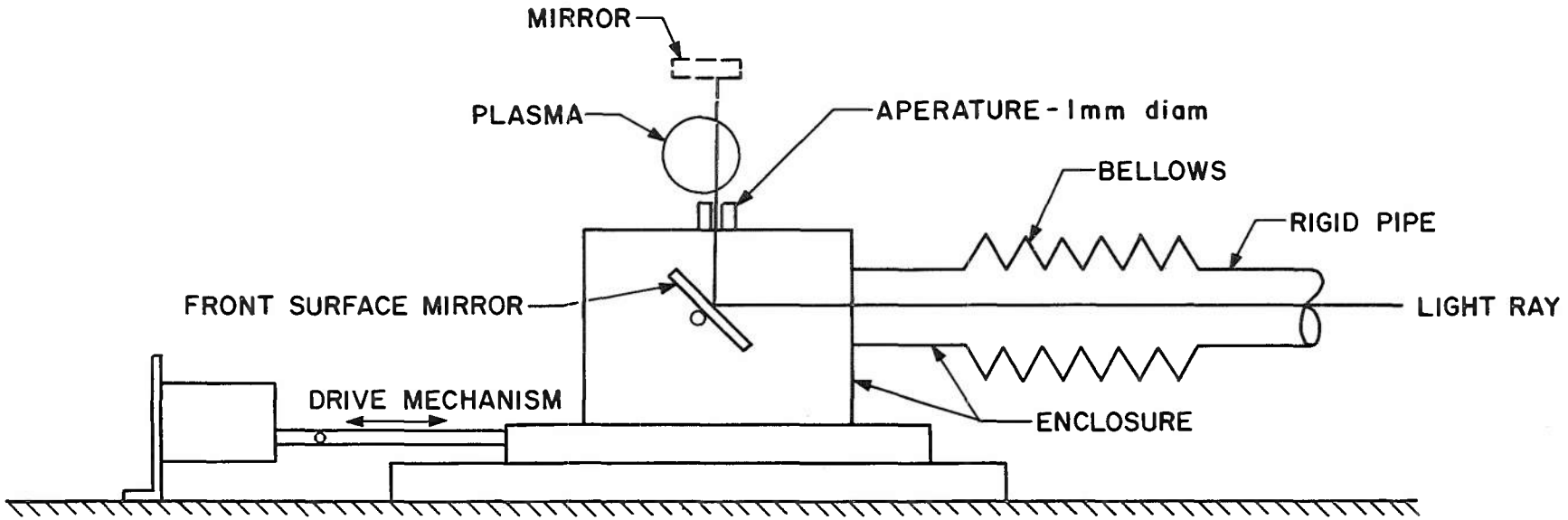

Fig. 6 Traversing Mechanism for Obtaining Spectral Intensity Profiles from a Side-On View of the Plasma Stream

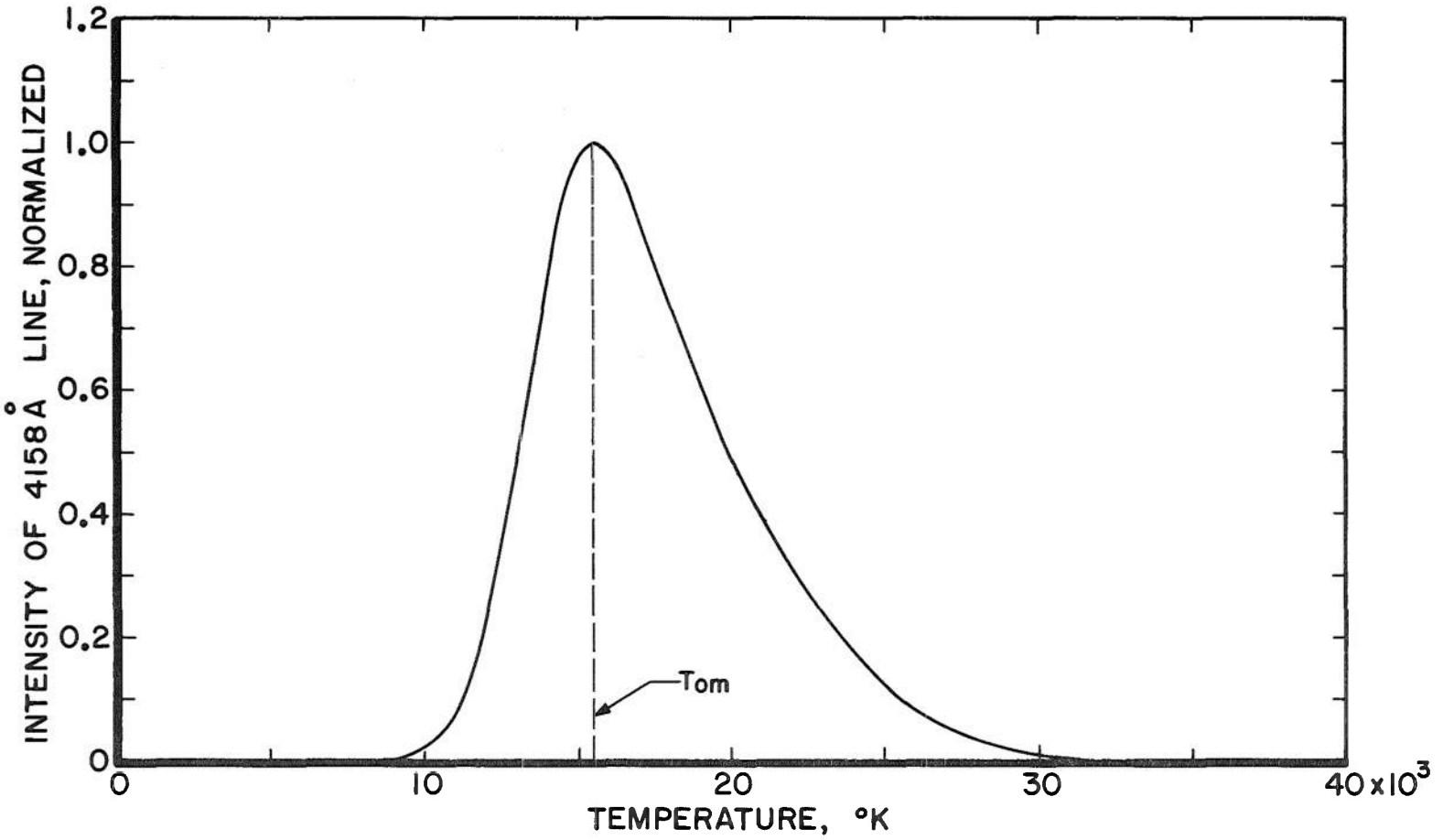

Fig. 7 Spectral Line Intensity of the 4158 Å Line of Argon as a Function of Temperature

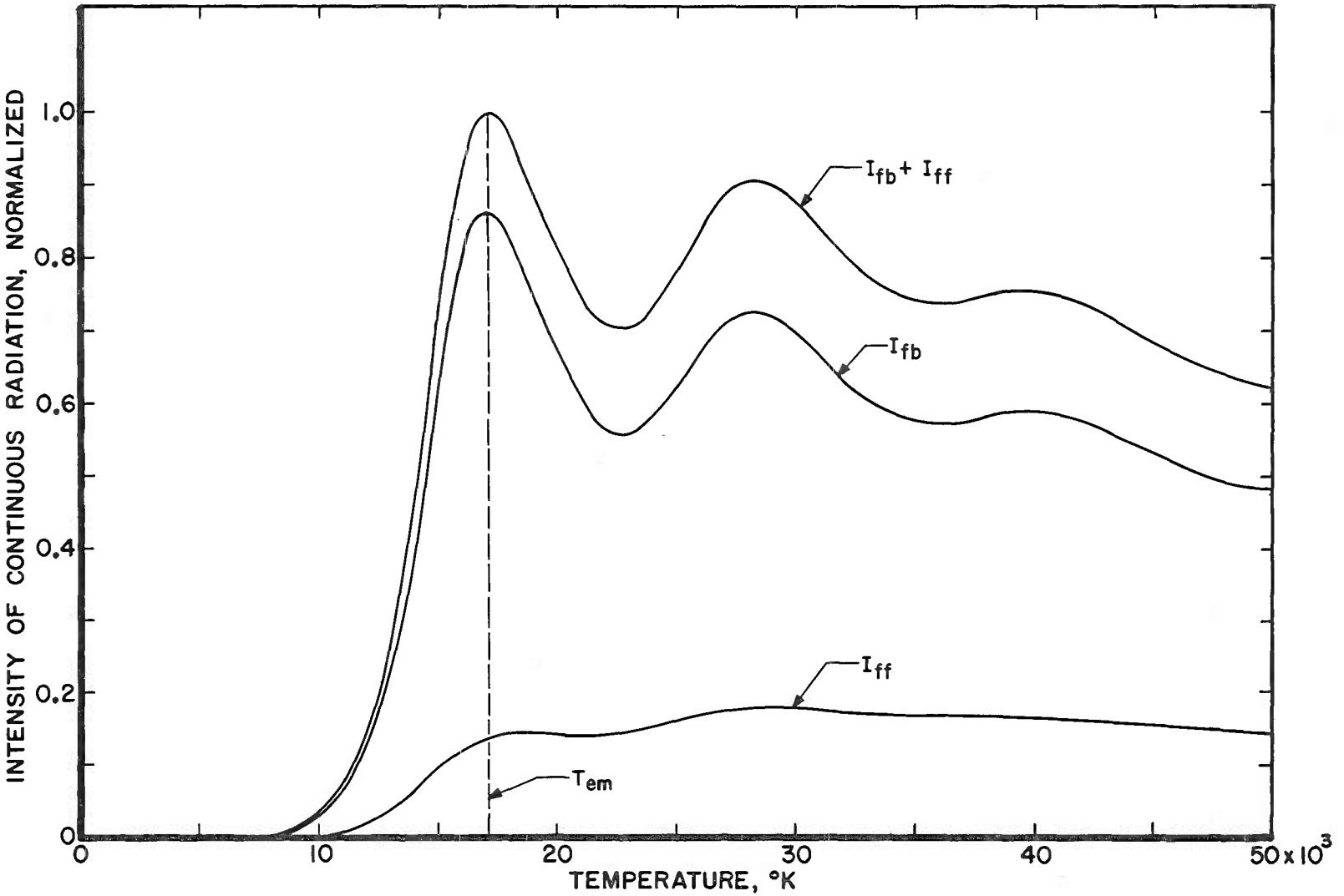

Fig. 8 Continuous Intensity at 4150 Å of the Radiation from Argon as a Function of Temperature

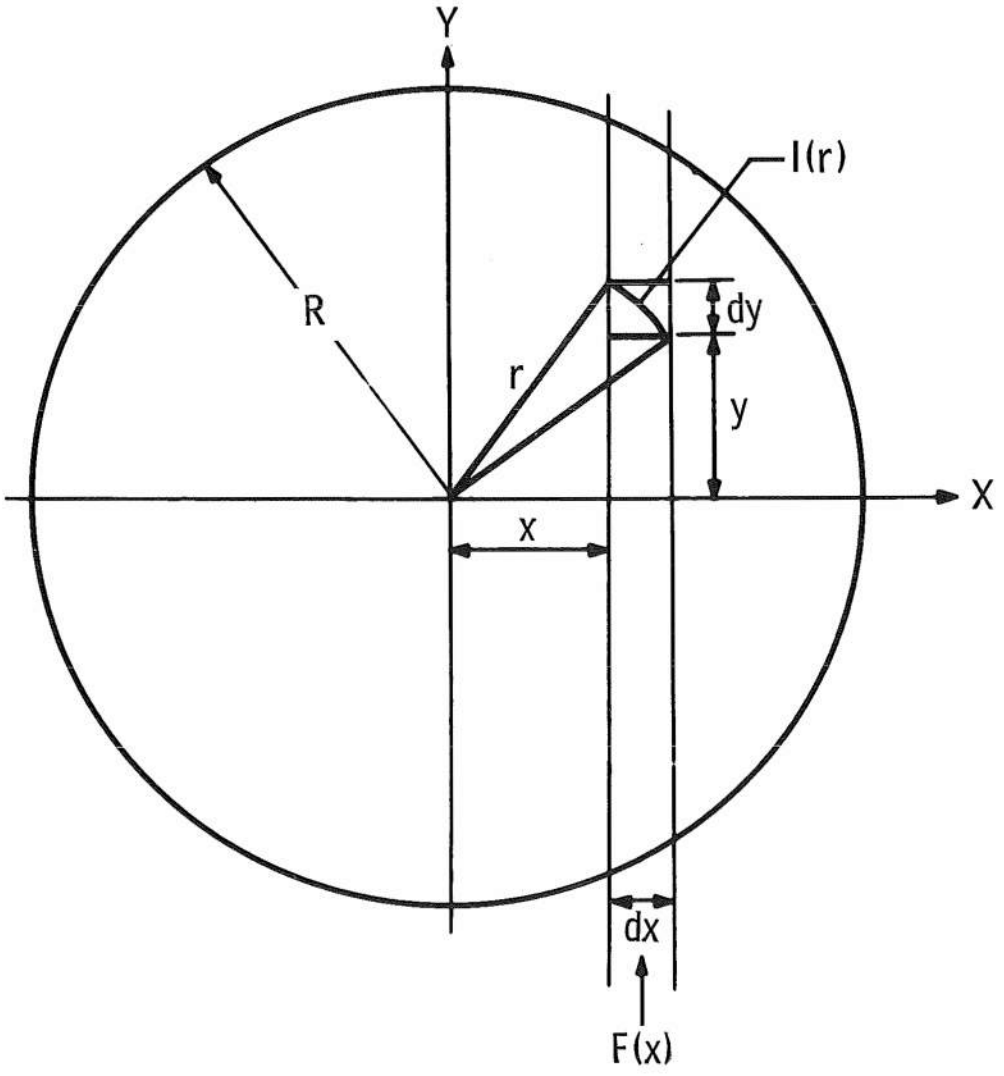

Fig. 9 Illustration of Lateral and Radial Intensity Distributions in an Axisymmetric Gas Stream

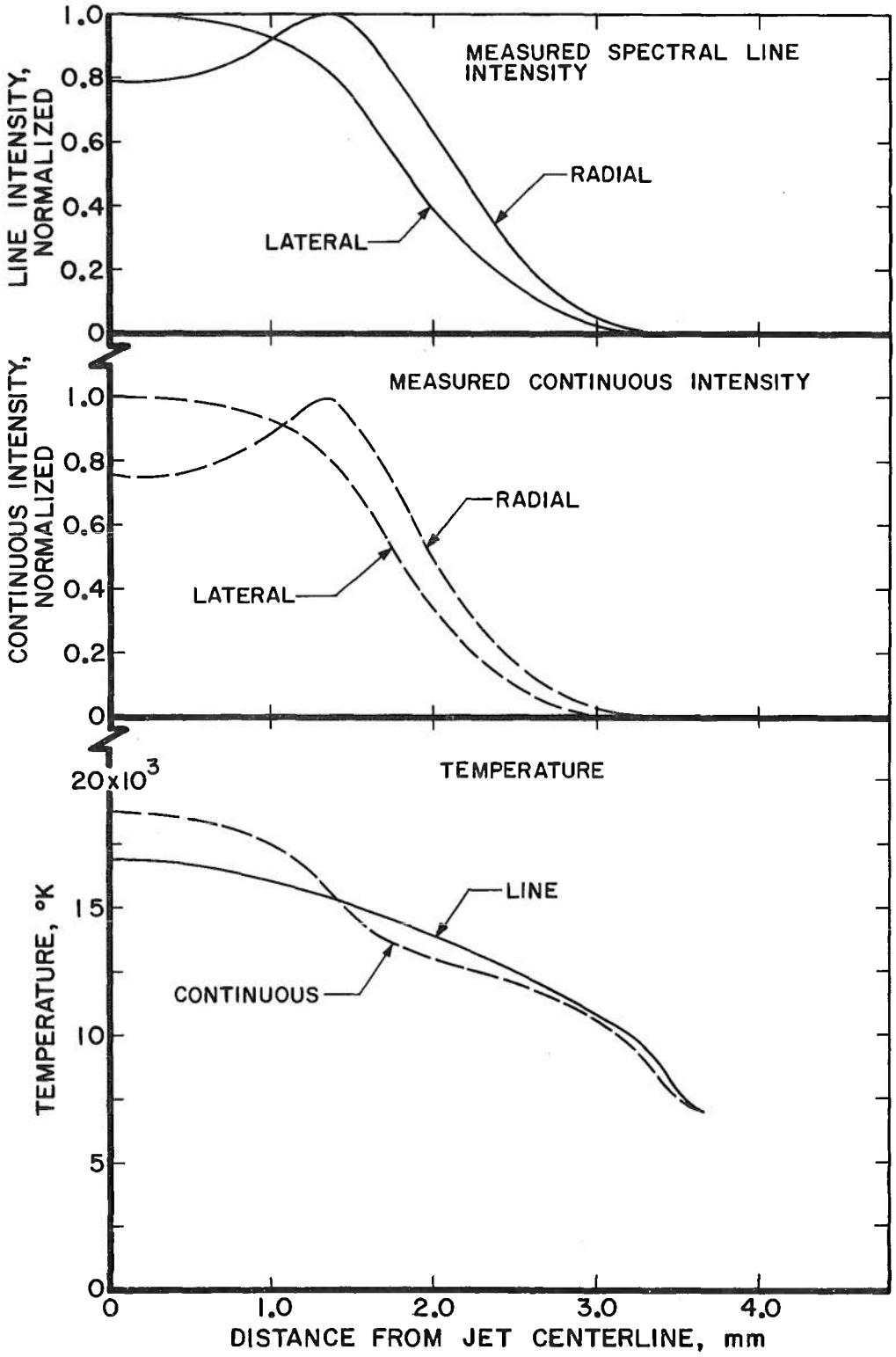

a. z = 6 mm

Fig. 10 Spectral Intensity and Temperature Profiles Obtained from the Plasma Stream – Operating Point 1 (Table 3)

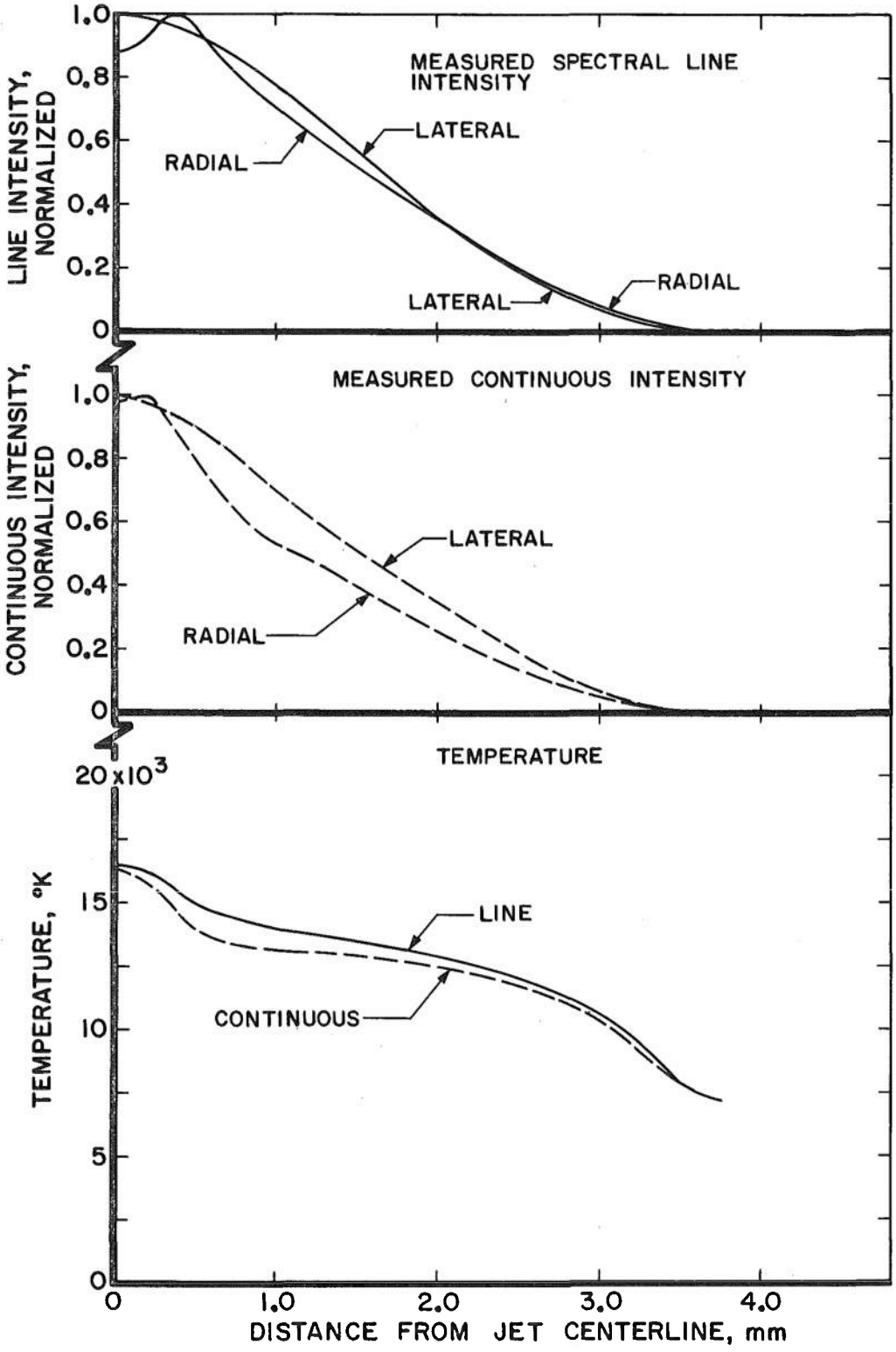

b. z = 19 mm

Fig. 10 Concluded

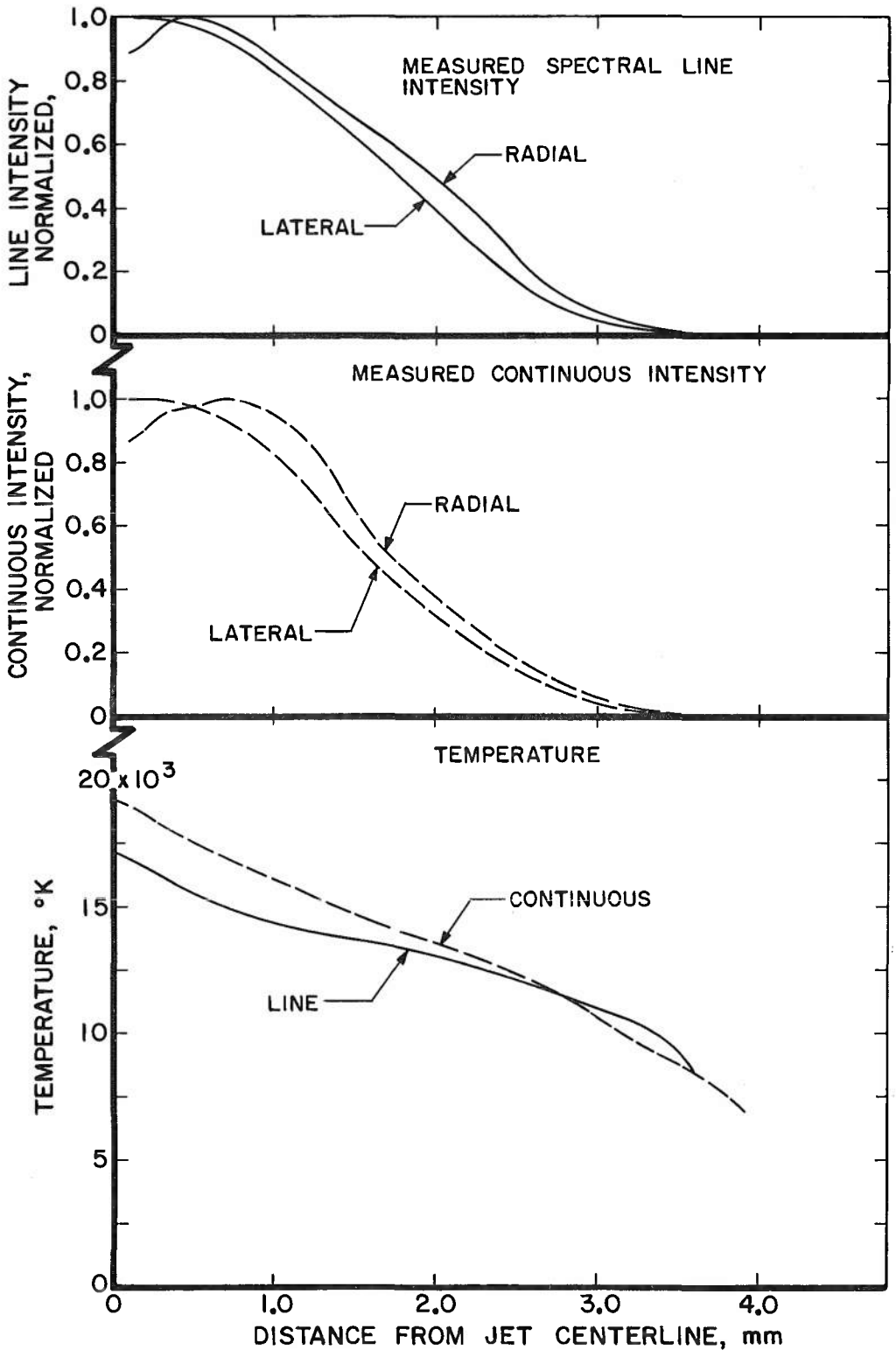

a. z = 3 mm

Fig. 11 Spectral Intensity and Temperature Profiles Obtained from the Plasma Stream – Operating Point 2 (Table 3)

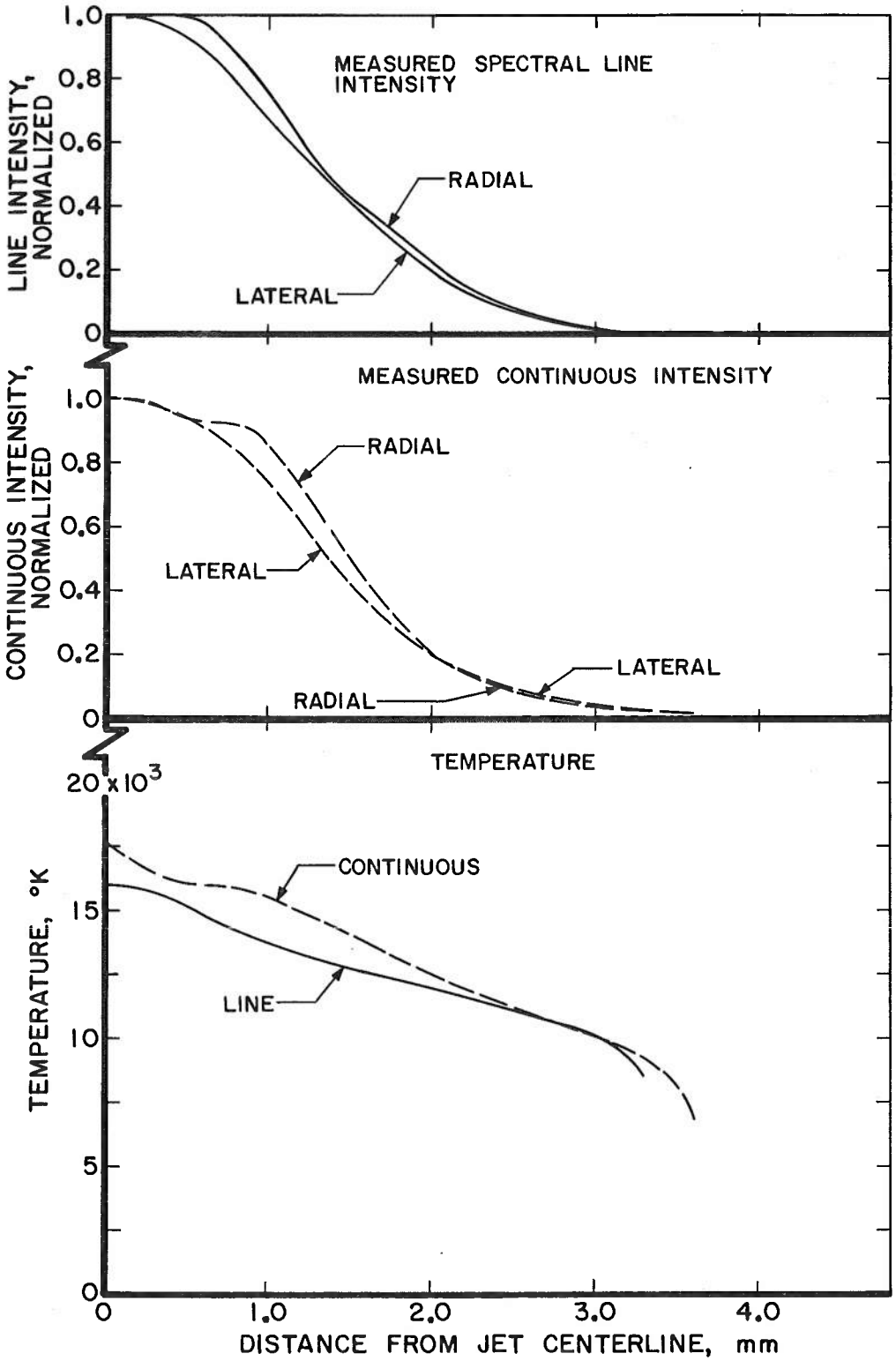

b. z = 10 mm

Fig. 11 Concluded

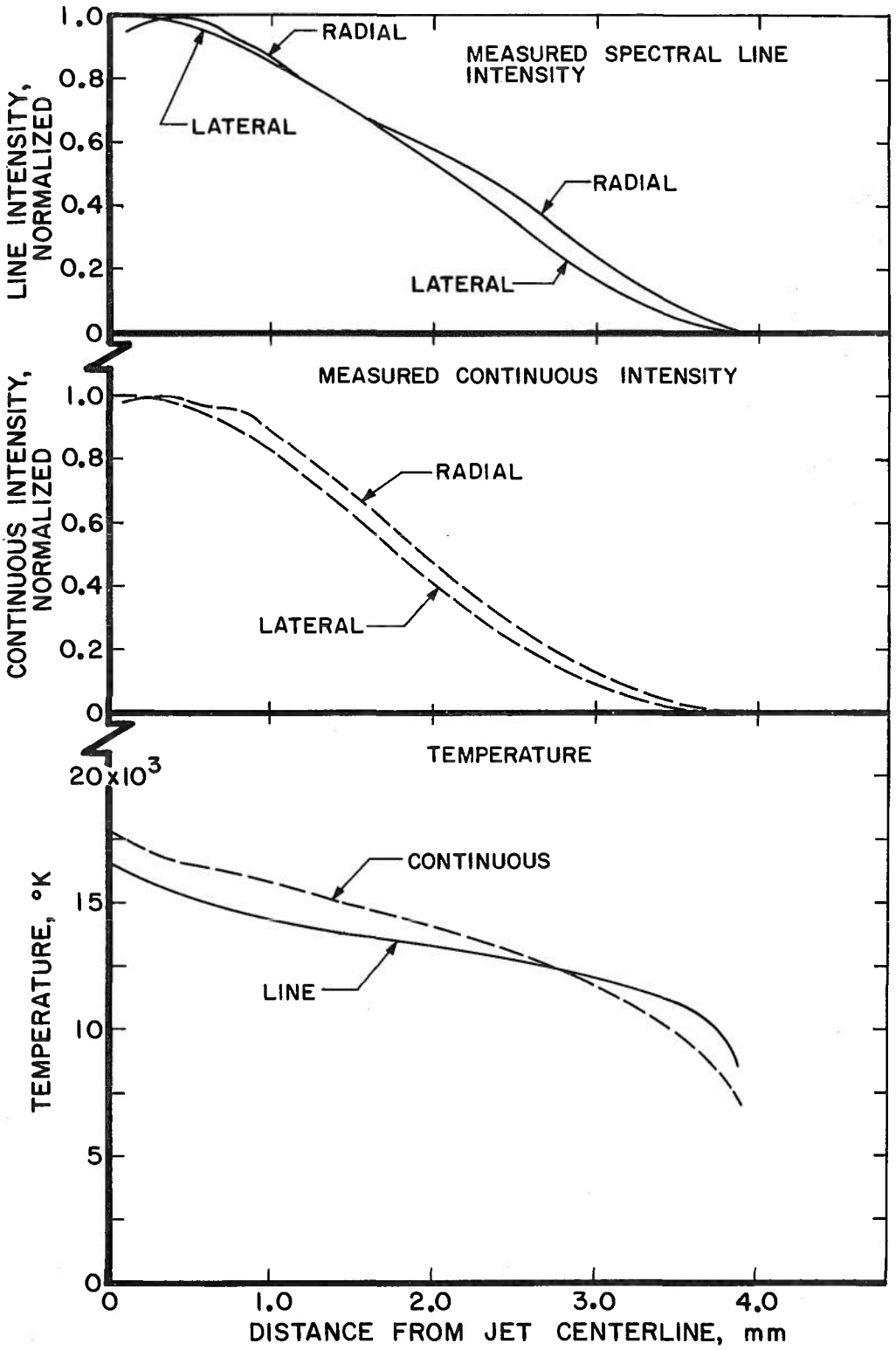

a. z = 3 mm

Fig. 12 Spectral Intensity and Temperature Profiles Obtained from the Plasma Stream – Operating Point 3 (Table 3)

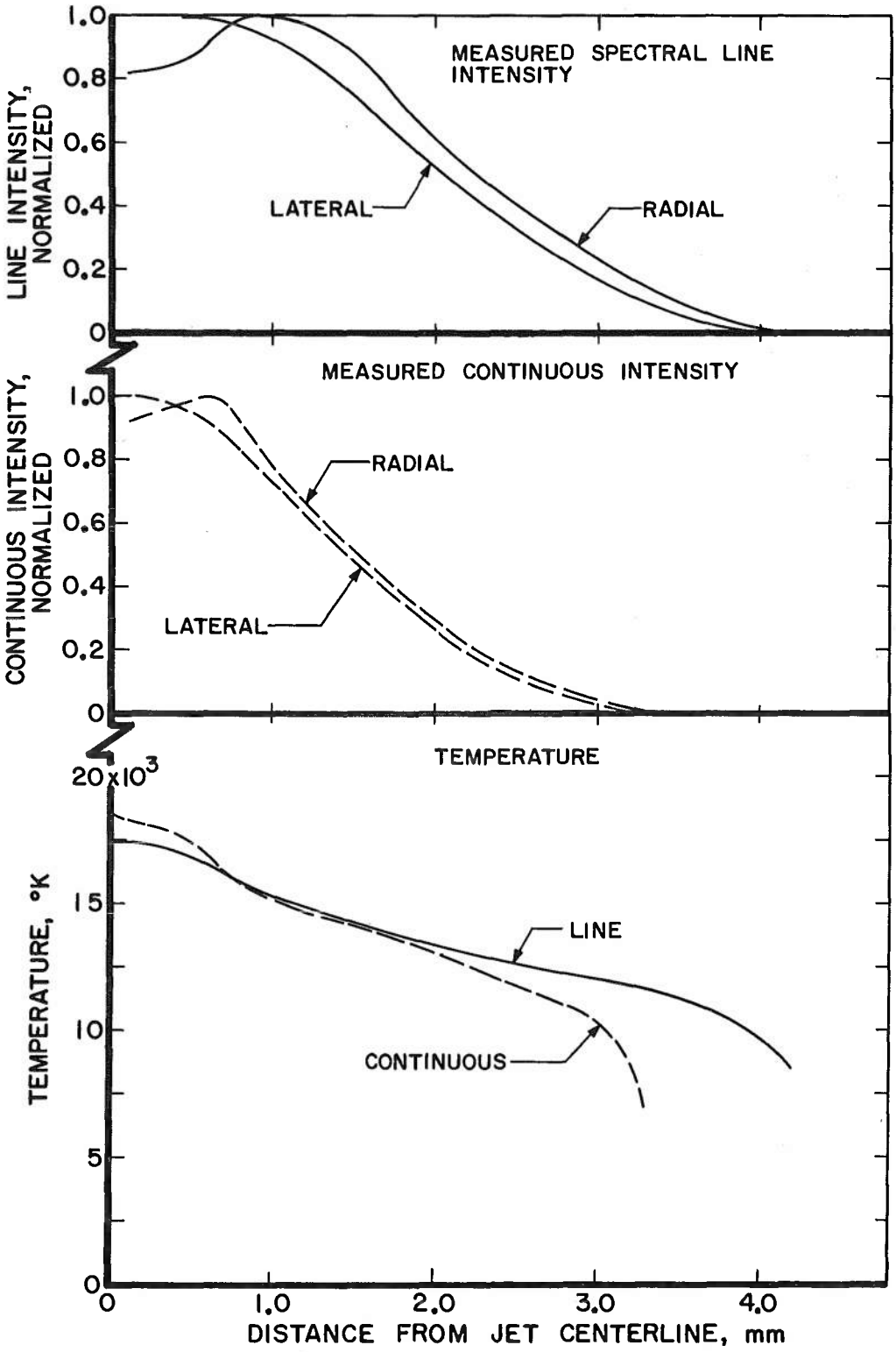

b. z = 10 mm

Fig. 12 Concluded

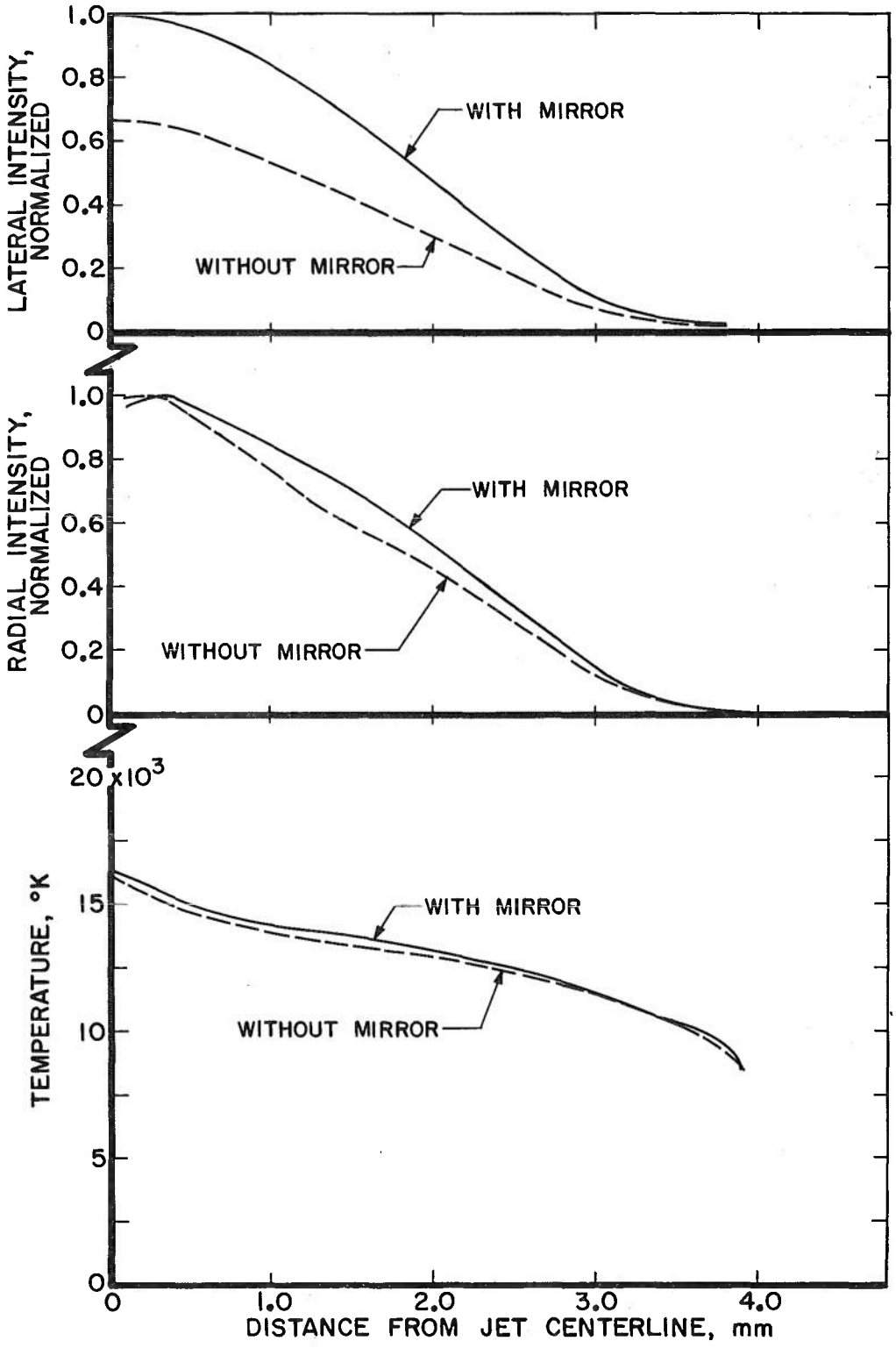

a. Spectral Line Emission

Fig. 13 Intensity and Temperature Profiles Obtained from the Plasma Stream to Demonstrate Whether Self-Absorption is Appreciable

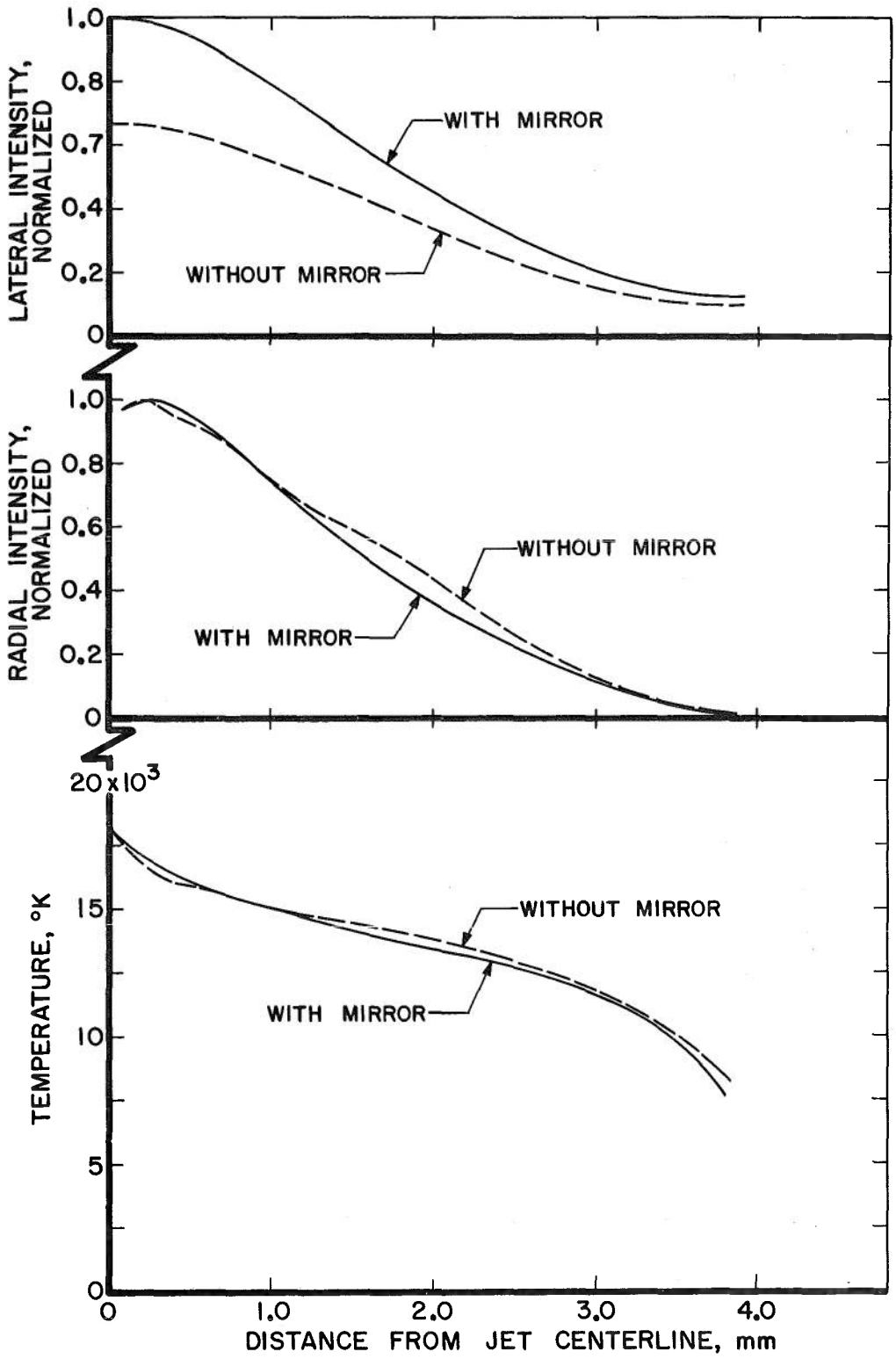

b. Continuous Emission

Fig. 13 Concluded

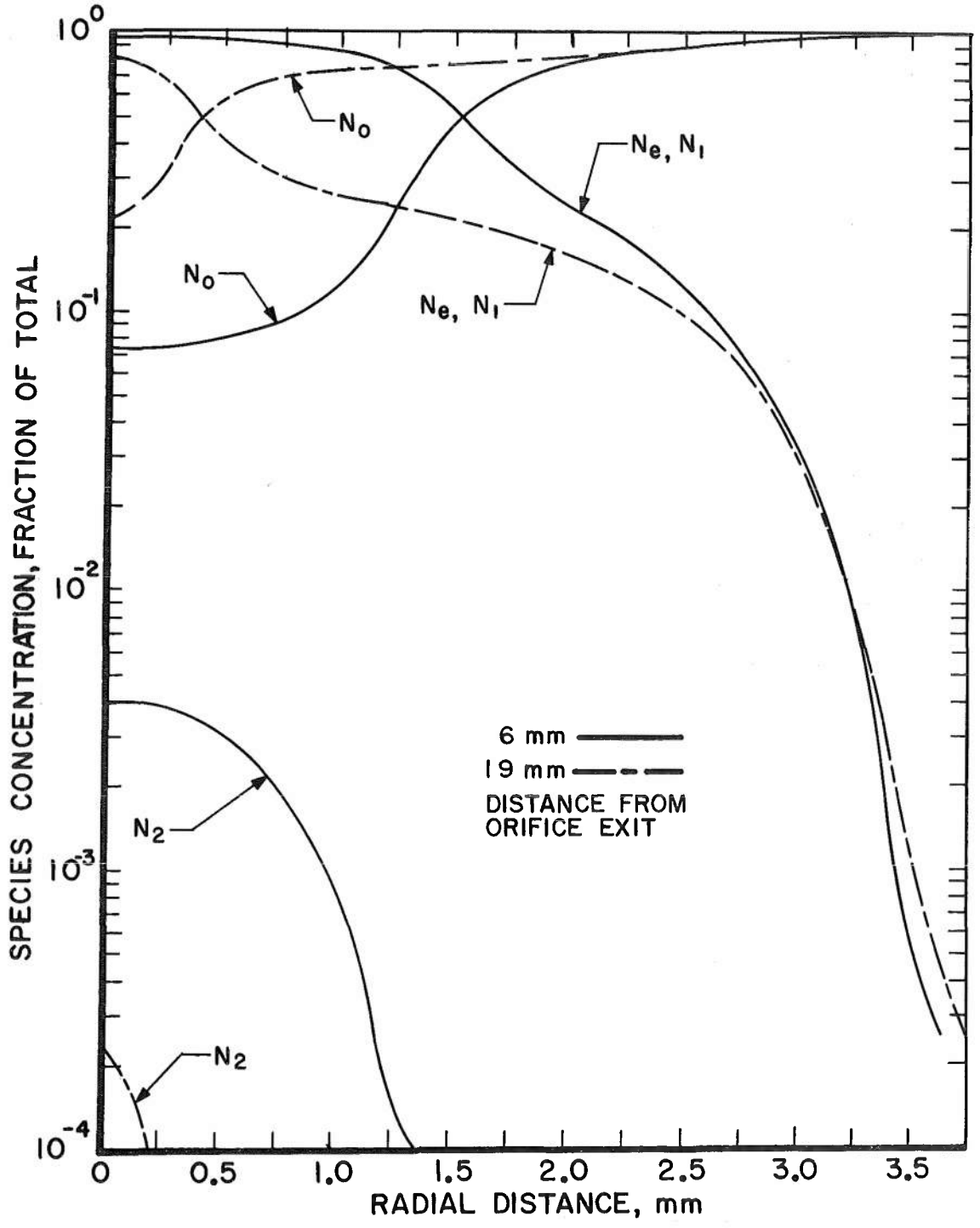

Fig. 14 Species Cancentratian Prafiles af the Plasma Stream Obtained by Application af the Saha Equatians ta the Temperature Prafiles af Fig. 10a

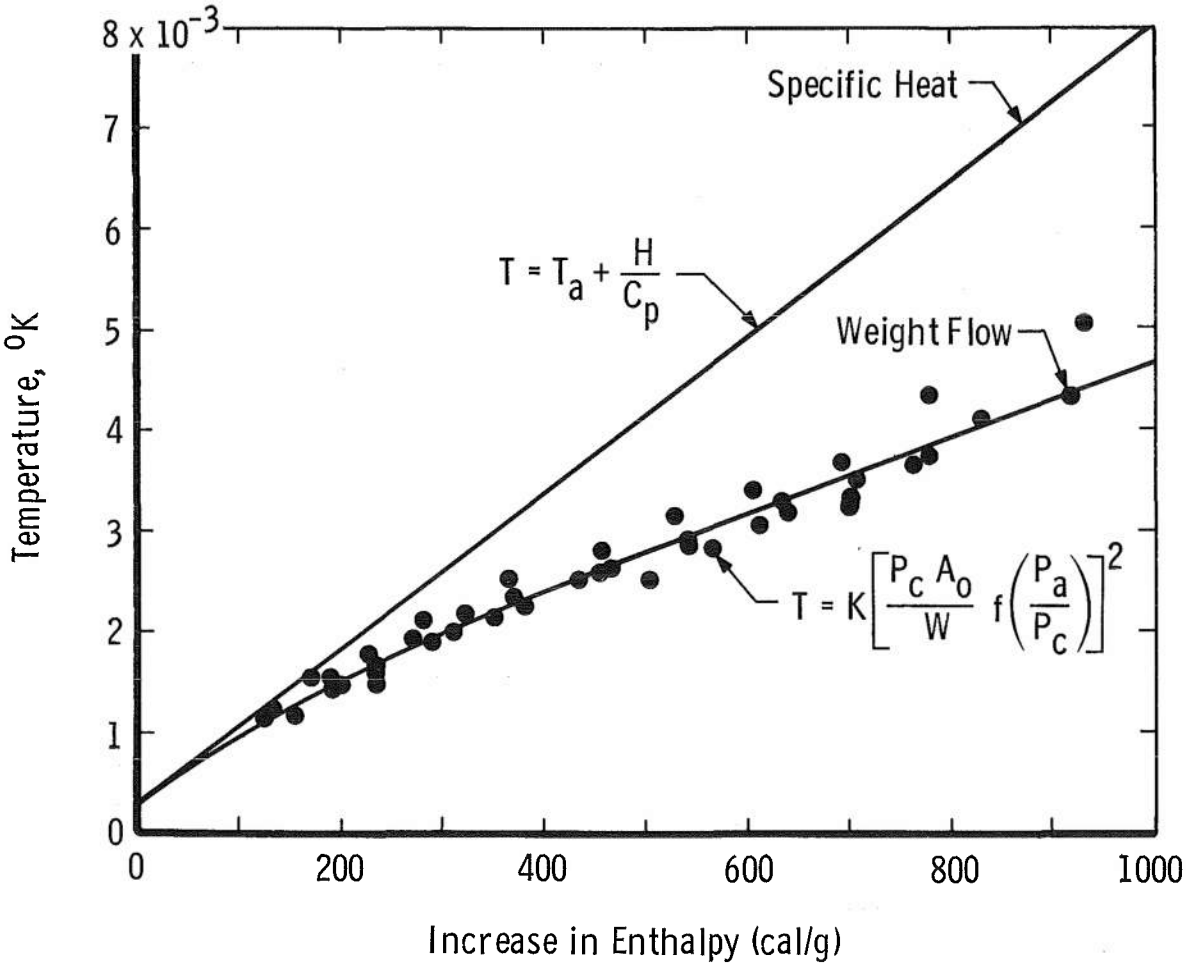

Fig. 15 Temperature Dependence an Specific Enthalpy far a Range of Plasma Generator Operatian

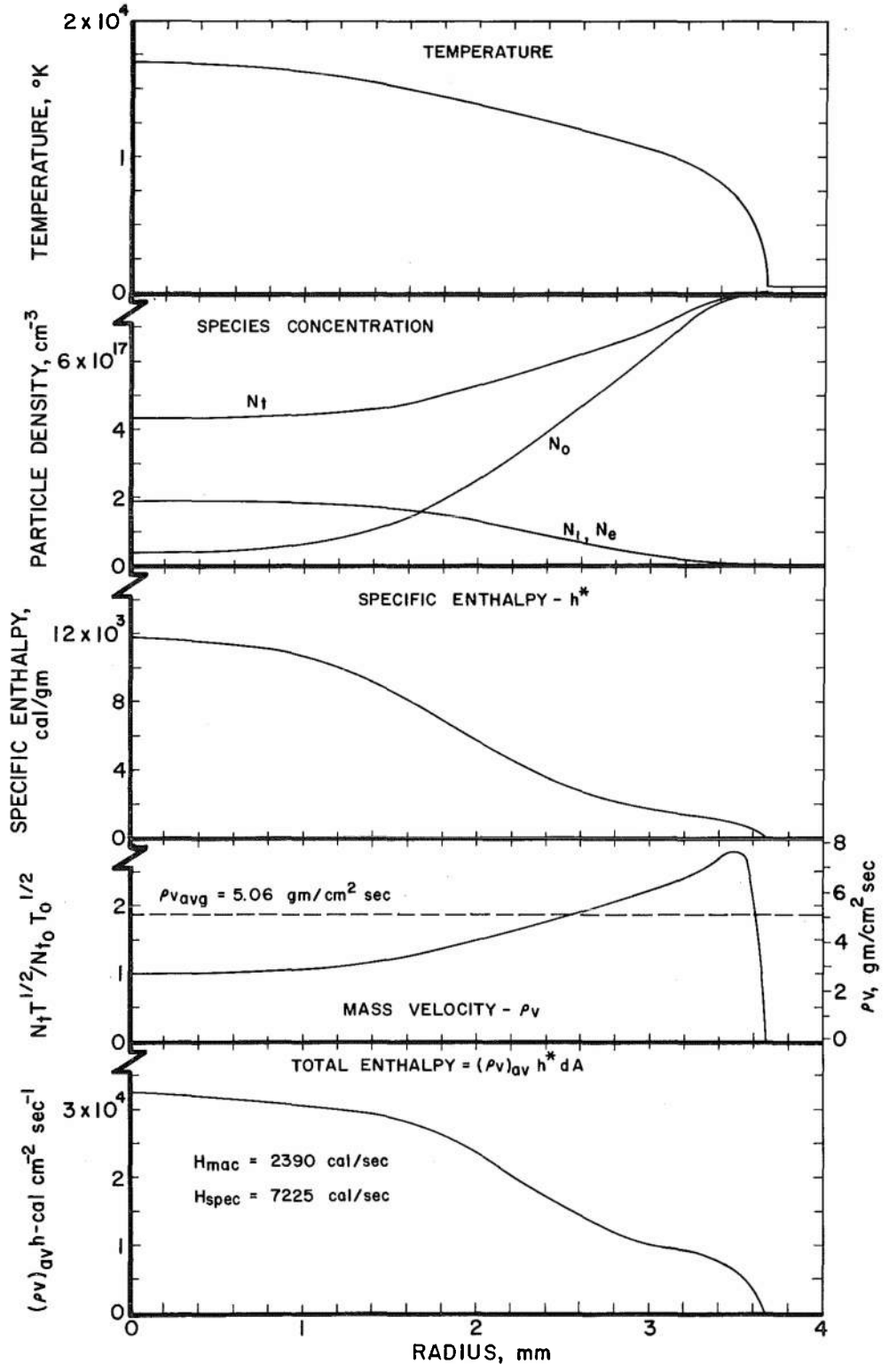

Fig. 16 Illustration of Total Enthalpy Determination from Spectrometric Data

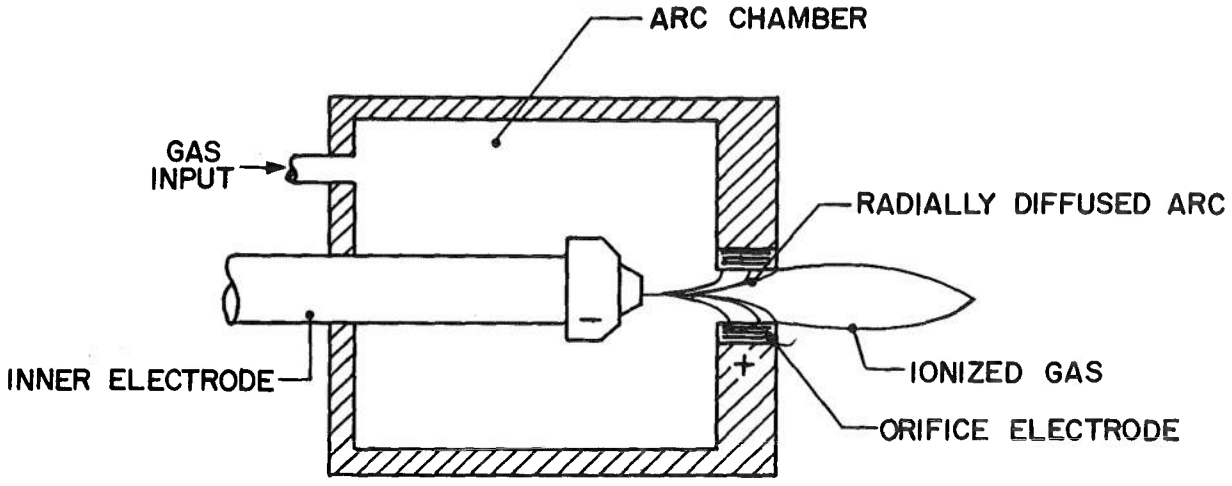

a. Rodiol Diffusion of Current

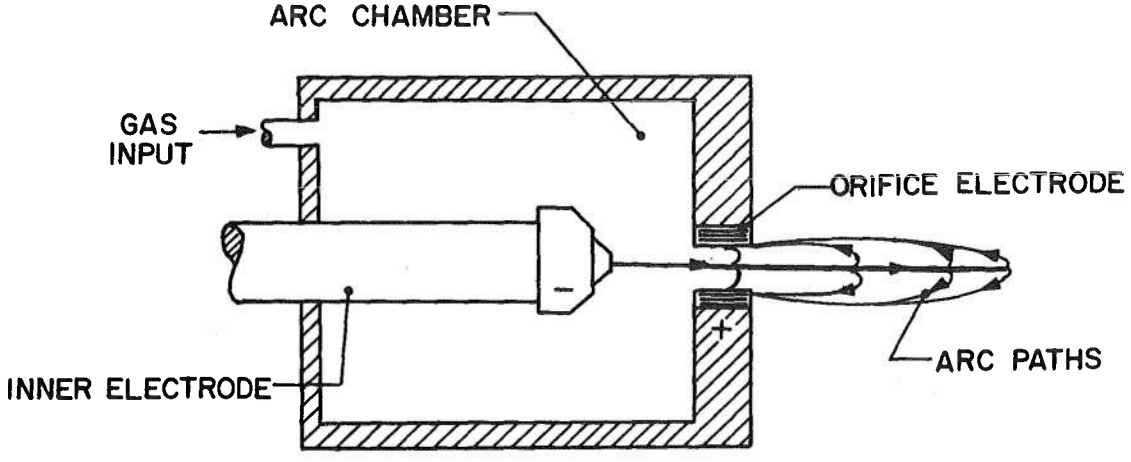

b. Externol Current Poths

Fig. 17 Illustrotion of Possible Arc Configurotions in a Gerdien-Electrode-Type Plosmo Generator

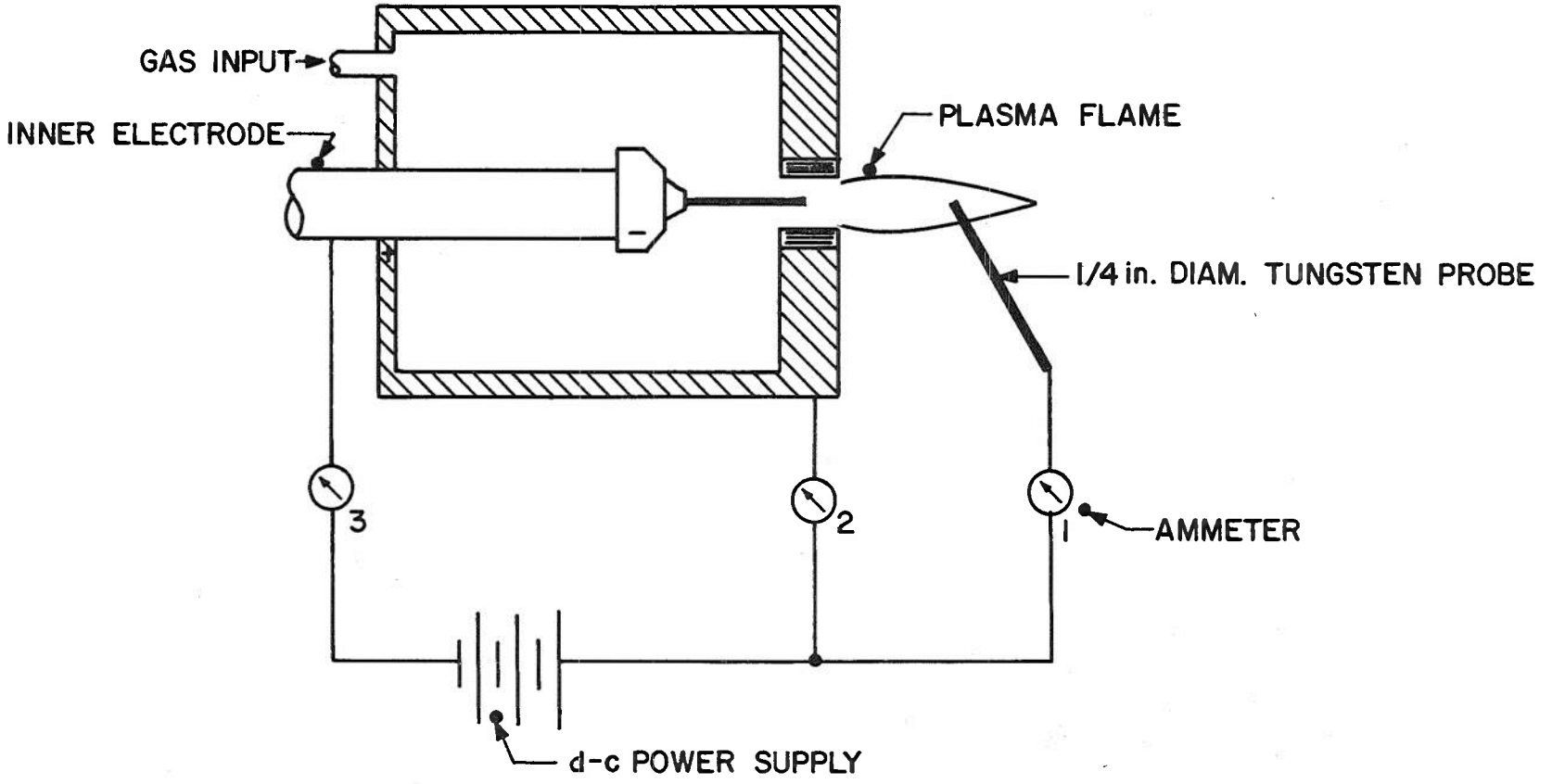

Fig. 18 Electrical Circuit for Probe Studies of the Plasma Stream

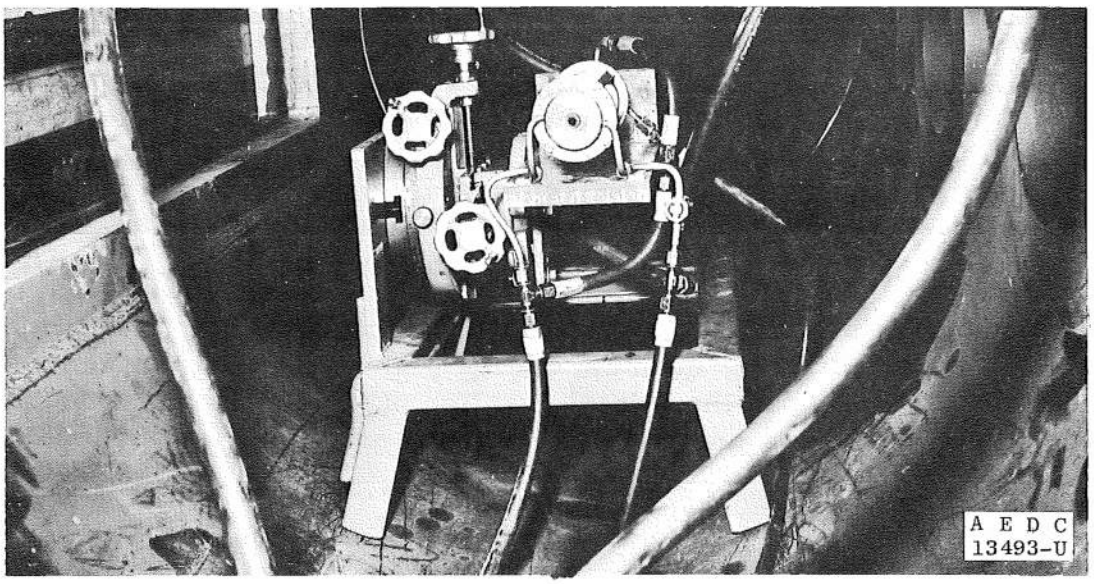

Fig. 19 Plasma Generator Installed in the Low Pressure Test Cell

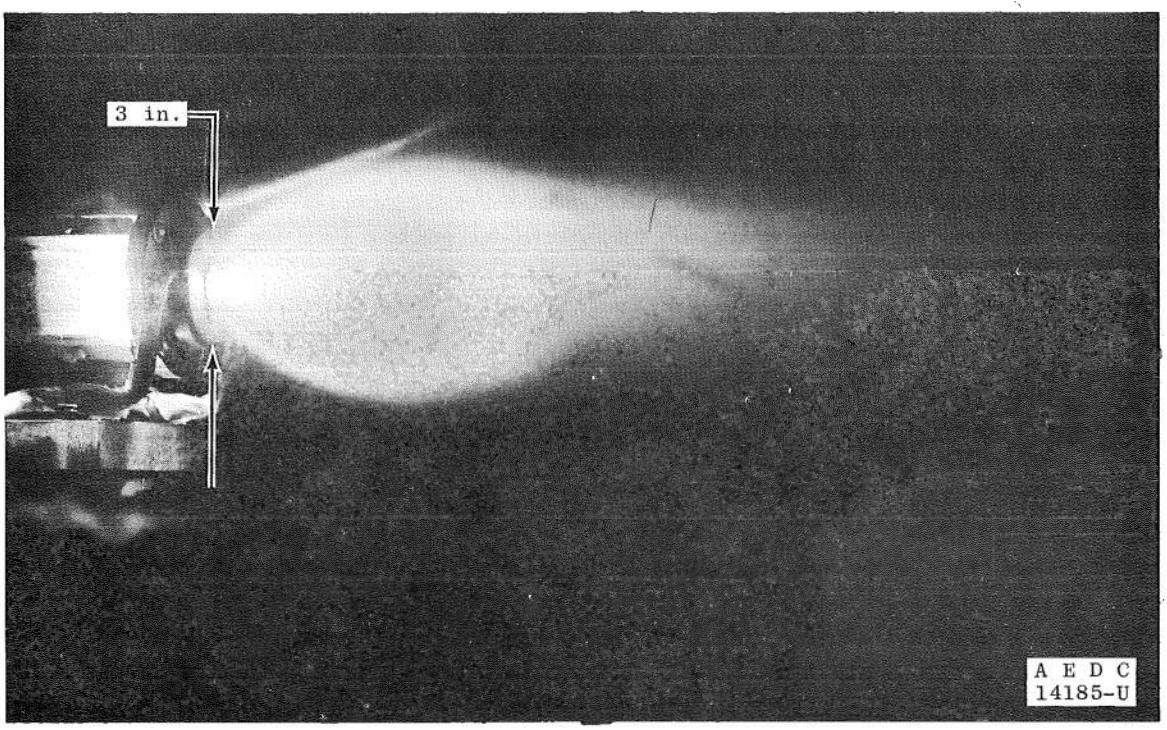

Fig. 20 Photograph of the Expanded Plasma Stream

APPENDIX A

CALCULATION OF ELECTRONIC PARTITION FUNCTION

The electronic partition function, U_r, appears in the Boltzmann energy distribution function which plays an important role in the formulas for spectral line intensities and also in the generalized Saha equations for species particle densities. It is expressed as

$$U_r = \sum_n g_{r,n} \exp\left(-\frac{E_{r,n}}{kT}\right) \tag{A1}$$

where the subscript r refers to the r^{th} state of ionization, $g_{r,n}$ is the statistical weight of the n^{th} quantum energy state, $E_{r,n}$ and is given by $g_{r,n} = 2J_{r,n} + 1$. $J_{r,n}$ is the orbital quantum number of the n^{th} state, k is the Boltzmann constant, and T is the absolute temperature. Numerically, the equation is

$$U_r = \sum_n g_{r,n} \exp\left(-1.439\ \frac{E_{r,n}}{T}\right) \tag{A2}$$

where $E_{r,n}$ is expressed in cm^{-1} and T is in °K. The summation must be taken over all the existing electronic states, and the major problem of this calculation is in this summation.

The energy of the $n = 0$ state is zero, and at temperatures less than about 12,000°K, the exponential terms for the neutral atom of argon differ from unity by less than 0.1 percent. For this reason,the partition function and the statistical weight (multiplicity of the first quantum level) are usually taken as being the same; that is, $U_o = g_{o,o}$. However, for higher temperatures, the summation of exponential terms begins to be appreciable and must be considered in the calculation. For the ionized species of argon where $E_{r,n}$ is much larger than $E_{o,n}$, the exponentials become appreciable, even at temperatures on the order of 5000°K.

If only the quantum energy states of atoms are considered, the summation of states, Eq. (A1), will not converge because there are an infinite number of energy states. In the actual case, the atom ionizes at some quantum level rather than proceeding to a higher quantum state. This gives justification, therefore, to cutting off the summation at some level, $n = i$. The difficulty arises in the choice of the cutoff level, i. Several criteria have been suggested for this choice, but so far they have been no better than an arbitrary choice. It suffices to say, for this work, that an arbitrary choice of 30 terms from the Bureau of Standards tables (Ref. 16) was used. The choice was based on a broad survey of the literature and seemed to represent a mean of the criteria used. The partition functions so calculated for argon are given in Fig. A1 for the neutral atom and five ionizations.

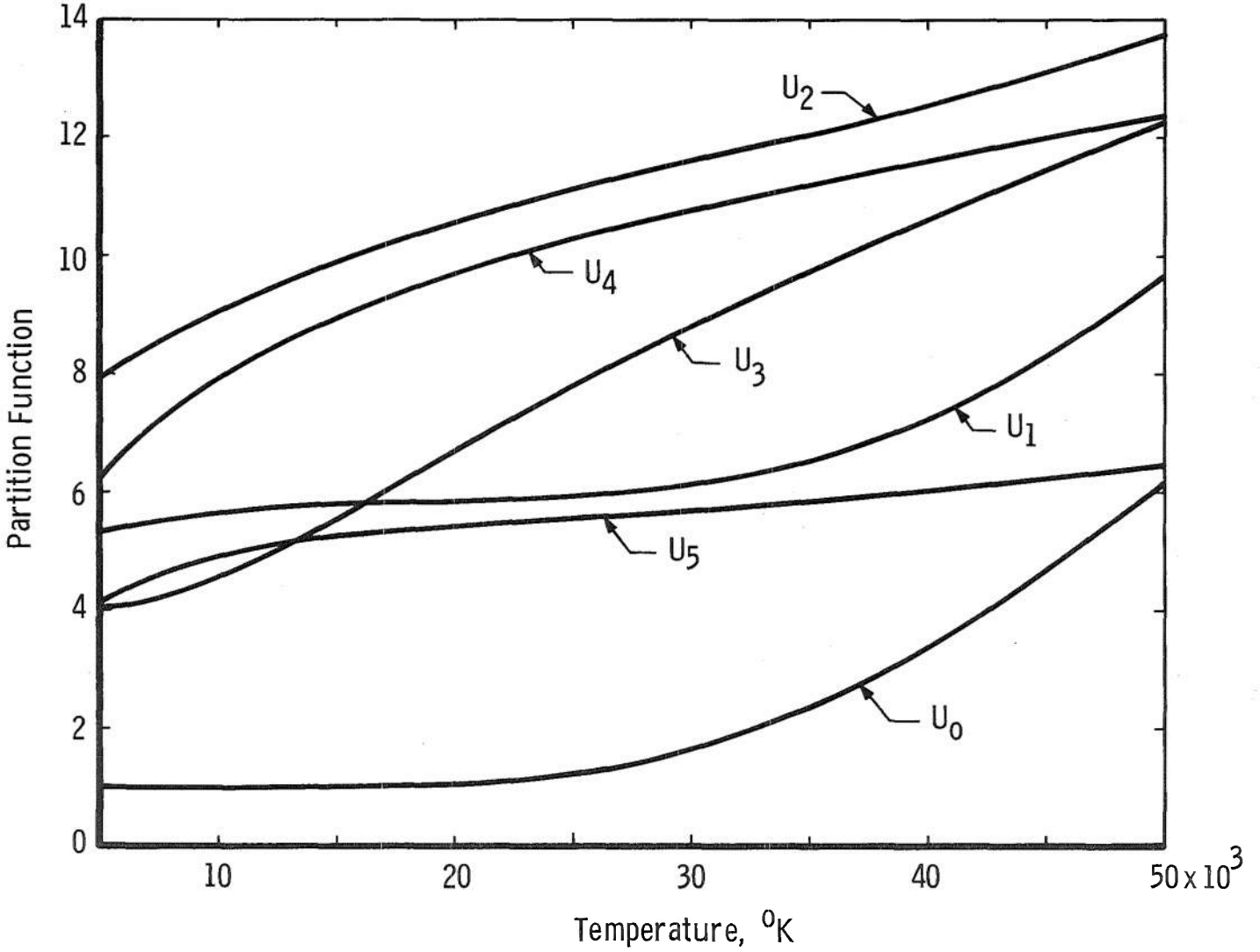

Fig. A1 Partition Functions for Neutral and Five Ionized States of Argon Obtained Using 30 Energy Terms

APPENDIX B

CALCULATION OF SPECIES CONCENTRATIONS

For the case of a perfect gas in a state of thermal equilibrium, the equilibrium constant for the reversible reaction

$$A_r \rightleftharpoons A_{r+1} + e - V_r \tag{B1}$$

where A_r is the initial particle, A_{r+1} is the next higher ionized particle, e is the free electron liberated, and V_r is the ionization energy, is given by

$$\frac{N_{r+1}\, N_e}{N_r} = \left(\frac{\sqrt{2\pi m_e k}}{h}\right)^3 \frac{2\, U_{r+1}}{U_r}\, T^{3/2} \exp\left(-\frac{V_r}{k\,T}\right) \tag{B2}$$

In Eq. (B2), N_{r+1}, N_r, and N_e are the particle densities of A_{r+1}, A_r, and e, respectively; m_e is the electron mass; k is the Boltzmann constant; h is Planck's constant; U_{r+1} and U_r are the partition functions of the A_{r+1} and A_r species, respectively; T is the absolute temperature of the gas; and V_r is the ionization potential required for the reaction, Eq. (B1). If r ionized species of an atom are to be considered, then r equations of the type, Eq. (B2), can be written. The equation of state for the perfect gas may be written

$$\frac{p}{k\,T} = N_t = N_o + N_1 + \cdots + N_r \cdots + N_e \tag{B3}$$

where p is the pressure. Also in an equilibrium gas the net charge must be neutral so that

$$N_e = N_i + 2N_2 + \cdots + rN_r + \cdots \tag{B4}$$

Equations (B2), (B3), and (B4) make up $r + 2$ equations, and there are $r + 2$ unknowns so that the set can be solved for the particle densities of all species and the electrons.

The equations necessary for the calculation of the first five ionizations of argon are as follows ($r = 5$ was chosen so that calculations would be accurate up to 50,000°K):

$$N_1 = \frac{N_o}{N_e} C_o \tag{B5}$$

$$N_2 = \frac{N_1}{N_e} C_1 \tag{B6}$$

$$N_3 = \frac{N_2}{N_e} C_2 \tag{B7}$$

$$N_4 = \frac{N_3}{N_e} C_3 \tag{B8}$$

$$N_5 = \frac{N_4}{N_e} C_4 \tag{B9}$$

$$N_e = N_1 + 2N_2 + 3N_3 + 4N_4 + 5N_5 \tag{B10}$$

$$\frac{p}{kT} = N_o + N_1 + N_2 + N_3 + N_4 + N_5 + N_e \tag{B11}$$

The parameters C are given by

$$C_r(T) = 4.8 \times 10^{15} \frac{U_{r+1}}{U_r} T^{3/2} \exp\left(-5040 \frac{V_r}{T}\right) \tag{B12}$$

where T is in °K and V_r is in volts. An IBM-7070 digital computer was used to solve this set of nonlinear algebraic equations for the species concentrations. The calculating procedure was

1. Select a value of T.
2. Calculate the values of C_r for that temperature using values for the partition functions from the calculations of Appendix A.
3. Using values of the species concentrations for the previous temperature as estimates, iterate until a solution is obtained.
4. Print out T and all N values, and proceed to a new value of T.

The species concentrations for argon for p = 1 are shown in Fig. B1.

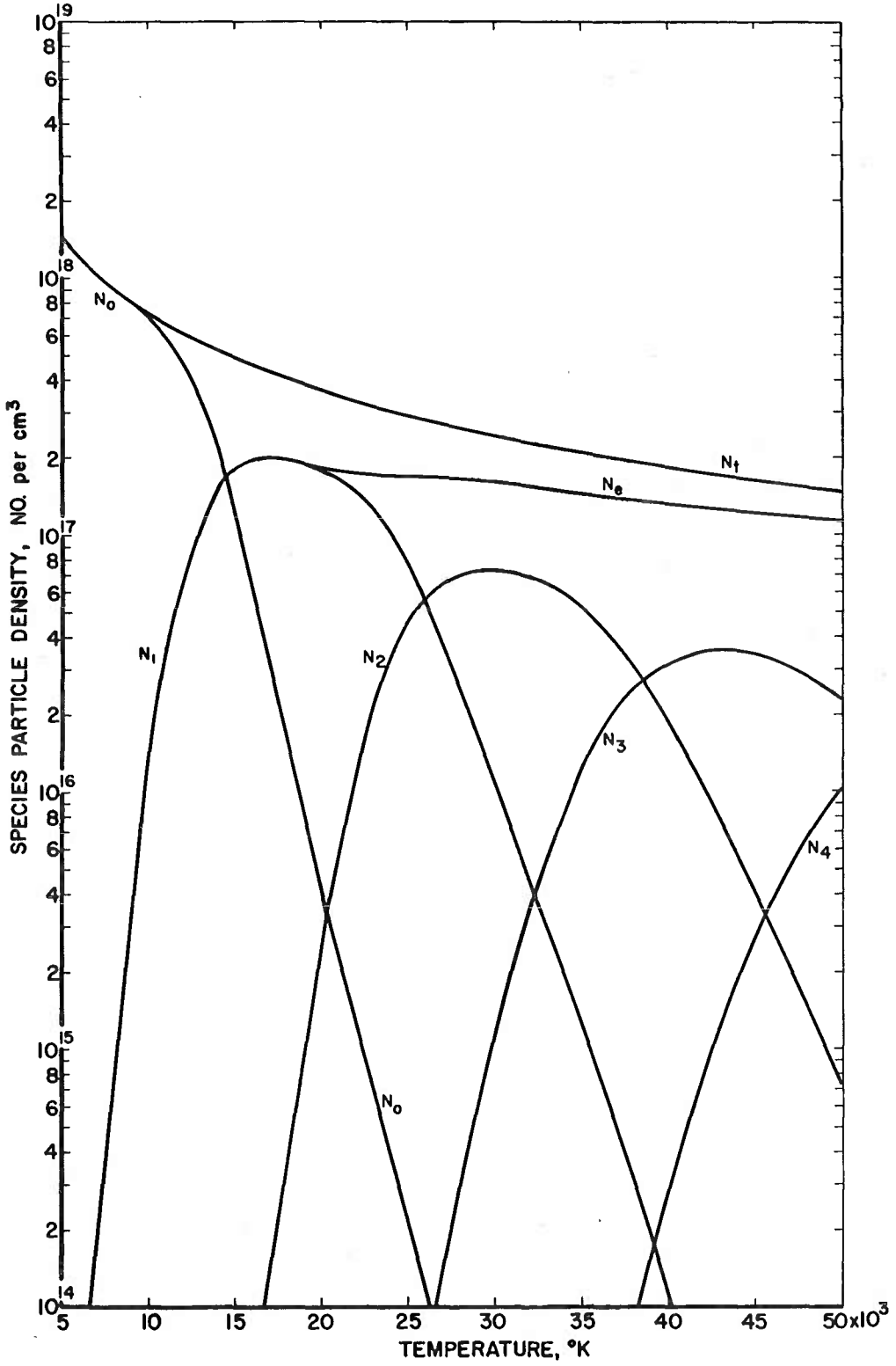

Fig. B1 Species Particle Densities for Argon as a Function of Temperature at One-Atmosphere Pressure

APPENDIX C

CALCULATION OF SPECIFIC ENTHALPY

The energy of a gas consists of translational, rotational, vibrational, and electronic portions (see Ref. 18 for a more complete treatment). The translational energy of a group, N_r, molecules, $\mathcal{E}_r^{tr}$, as determined from kinetic theory, is

$$\mathcal{E}_r^{tr} = \frac{3}{2} N_r k T \tag{C1}$$

where T is the absolute temperature and k is Boltzmann's constant. For monatomic gases, the rotational and vibrational states do not exist, and the electronic energy is divided among electron quantum states, each with energy, $E_{r,n}$. At equilibrium the Maxwell-Boltzmann distribution law relates the number of atoms of the species, r, in the n^{th} quantum state, $N_{r,n}$, to the number in the ground ($E_{r,o} = 0$) state, $N_{r,o}$,

$$N_{r,n} = N_{r,o} \exp\left(-\frac{E_{r,n}}{kT}\right) \tag{C2}$$

The total number of atoms per cm^3 of the r^{th} species, N_r, is then

$$N_r = N_{r,o} \sum_n g_{r,n} \exp\left(-\frac{E_{r,n}}{kT}\right) \tag{C3}$$

where $g_{r,n}$ is the multiplicity of the level, $E_{r,n}$. The total energy in the electronic states is the sum of the product of the state times the number in that state,

$$\mathcal{E}_r^e = \sum_n N_{r,n} E_{r,n} = N_{r,o} \sum_n g_{r,n} E_{r,n} \exp\left(-\frac{E_{r,n}}{kT}\right) \tag{C4}$$

or, substituting for $N_{r,o}$ from Eq. (C3) into Eq. (C4)

$$\mathcal{E}_r^e = N_r \frac{\sum_n g_{r,n} E_{r,n} \exp\left(-\frac{E_{r,n}}{kT}\right)}{\sum_n g_{r,n} \exp\left(-\frac{E_{r,n}}{kT}\right)} \tag{C5}$$

Now, because the denominator is only the partition function,

$$U_r = \sum_n g_{r,n} \exp\left(-\frac{E_{r,n}}{kT}\right)$$

Eq. (C5) can be written

$$\mathcal{E}_r^e = \frac{N_r}{U_r} \sum_n g_{r,n} E_{r,n} \exp\left(-\frac{E_{r,n}}{kT}\right) \tag{C6}$$

Equations (C1) and (C6) give the total translational and electronic energy above a reference temperature (absolute zero in this case),

respectively, of a monatomic gas consisting of a group $\sum_r N_r$ molecules. The ionization energy, $\mathcal{E}_r^i$, must be added also to account for the energy required to form the species, r. The total energy contained by the N_r molecules is then

$$\mathcal{E}_r^{total} = \mathcal{E}_r^{tr} + \mathcal{E}_r^{e} + \mathcal{E}_r^{i} \tag{C7}$$

Dividing Eq. (C7) by N_r and substituting for the energy terms

$$e_r^{total} = \frac{\mathcal{E}_r^{total}}{N_r} = \frac{3}{2} kT + \frac{1}{U_r} \sum_n g_{r,n} E_{r,n} \exp\left(-\frac{E_{r,n}}{kT}\right) + e_r^i \tag{C8}$$

This is the total energy per molecule or specific internal energy of the species r. The specific enthalpy, h*, is related to specific internal energy by $e = h^* - kT$ and is expressible as

$$h_r^{total} = \frac{5}{2} kT + \frac{1}{U_r} \sum_n g_{r,n} E_{r,n} \exp\left(-\frac{E_{r,n}}{kT}\right) + e_r^i \tag{C9}$$

All the thermodynamic properties of a monatomic gas can be evaluated from Eqs. (C8) and (C9). The specific heat per molecule at constant volume, c_v, of the r species is given by

$$c_v = \frac{\partial}{\partial T}\left(e_r^{total}\right) = \frac{3}{2} k + \frac{1}{kT^2} \frac{\sum_n g_{r,n} (E_{r,n})^2 \exp\left(-\frac{E_{r,n}}{kT}\right)}{\sum_n g_{r,n} \exp\left(-\frac{E_{r,n}}{kT}\right)} - \frac{\left[\sum_n g_{r,n} E_{r,n} \exp\left(-\frac{E_{r,n}}{kT}\right)\right]^2}{\left[\sum_n g_{r,n} \exp\left(-\frac{E_{r,n}}{kT}\right)\right]} \tag{C10}$$

and the specific heat at constant pressure, c_p, is given by

$$c_p = \frac{\partial}{\partial T}\left(h_r^{total}\right) = c_v + k \tag{C11}$$

It suffices here to calculate h_r^{total} for each of six species of argon. The ionization energies e_r^i are given as follows where the energy units are cm^{-1} per particle.

$e_o^i = 0$ $\qquad$ $e_3^i = 329{,}966$

$e_1^i = 127{,}110$ $\qquad$ $e_4^i = 482{,}400$

$e_2^i = 222{,}820$ $\qquad$ $e_5^i = 605{,}100$

The results of the calculation of the specific enthalpy of argon are shown in Fig. C1. Spectrometric units were used for the energy terms because

these are the convenient units for our purposes. A convenient conversion factor is cm^{-1} times 4.75×10^{-24} equals calories. To calculate the average specific enthalpy for a gas at a given temperature, the species concentrations (see Appendix B) must also be known. Then

$$h_{avg} = \frac{\sum_r N_r h_r}{\sum_r N_r} \tag{C12}$$

where N_r is obtained from Fig. B1. The average specific enthalpy is shown in Fig. C2.

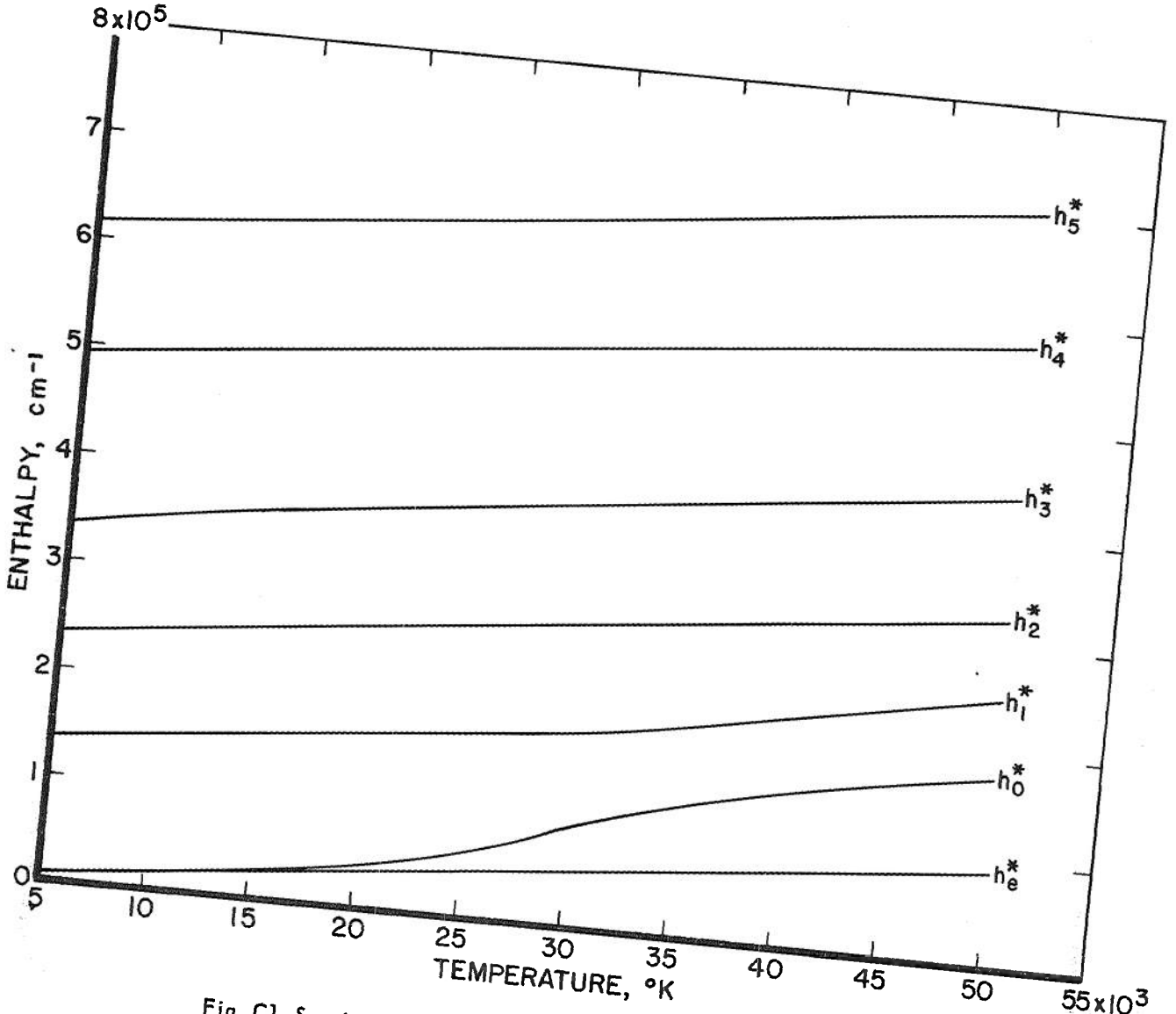

Fig. C1 Species Specific Enthalpy for Argon at High Temperatures

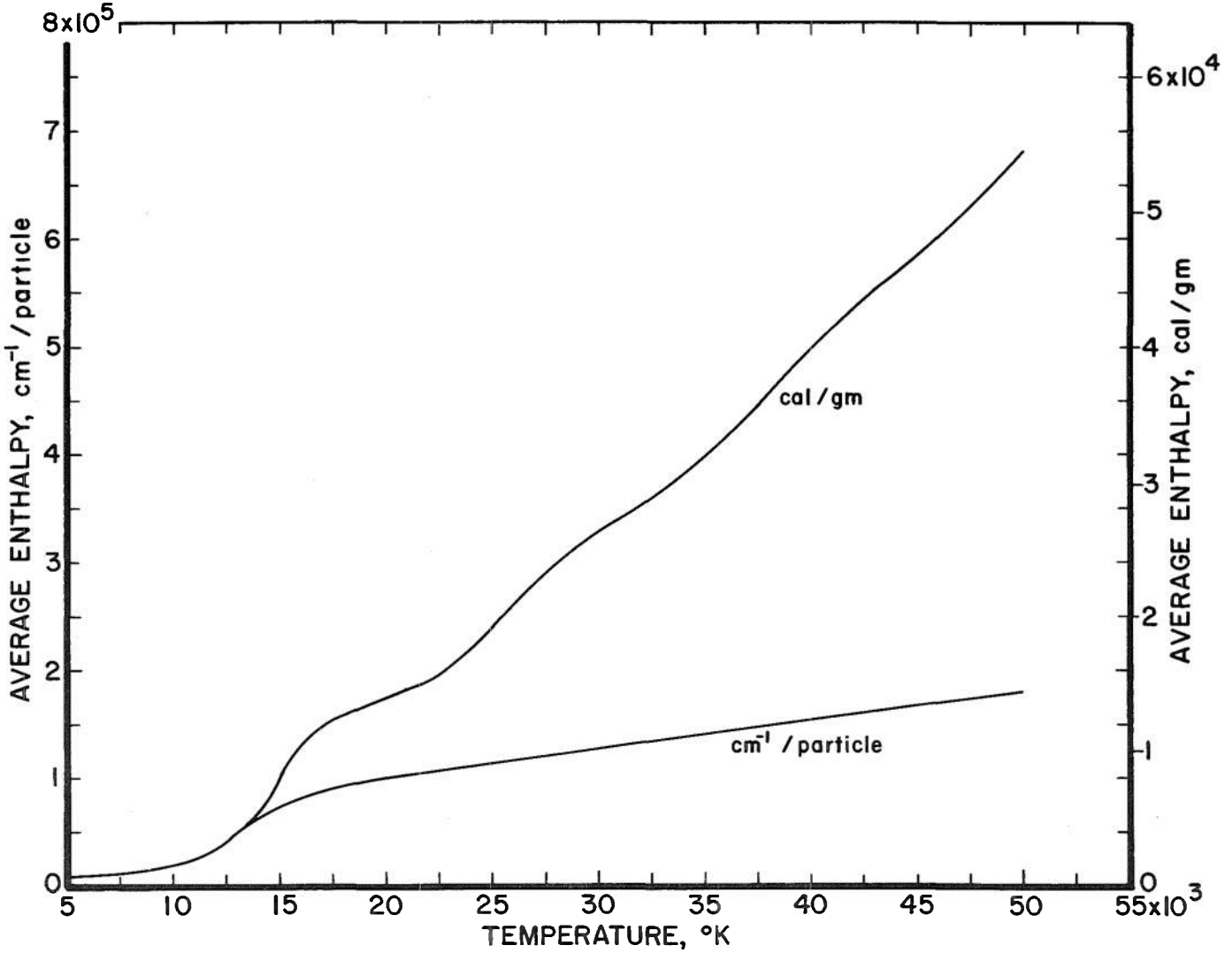

Fig. C2 Average Specific Enthalpy for Argon at High Temperotures